

## Review

## Carbon dots-based delayed fluorescent materials: Mechanism, structural regulation and application

Mingxiu Lei,<sup>1</sup> Jingxia Zheng,<sup>1</sup> Yongzhen Yang,<sup>1,\*</sup> Lingpeng Yan,<sup>1,2,\*</sup> Xuguang Liu,<sup>2</sup> and Bingshe Xu<sup>1,3</sup>

## SUMMARY

**Delayed fluorescent (DF) materials have high internal quantum efficiency because of the triplet excitons involved in the radiation transition, and the spin-forbidden transition can effectively improve their luminescent lifetime. Compared with traditional afterglow materials including metal-containing inorganic coordination compounds and organic compounds, the DF materials based on carbon dots (CDs) have drawn extensive attention because of their advantages of low toxicity, environmental friendliness, stable luminescence, easy preparation and low cost. Most CDs-based DF materials can be realized by embedding CDs in matrix with covalent bonds, hydrogen bonds or/and other supramolecular interactions. Recently, matrix-free self-protective CDs-based DF materials are emerging. This review systematically summarizes the DF mechanism and structural regulation strategies of CDs-based DF materials, and the applications of CDs-based DF materials in anti-counterfeiting, information encryption, temperature sensing and other fields are introduced. Finally, the existing problems and future potentials of CDs-based DF materials are proposed and prospected.**

## INTRODUCTION

Luminescent materials are of increasing importance in the energy industry and have shown growing demand in intelligent sensor, security printing, solar cells, and other fields besides display lighting (Jiang et al., 2020a; Xing et al., 2020; Zhao et al., 2020a; Zhou et al., 2017; Li et al., 2017; Zhuo and Brgoch, 2021). The development of advanced luminescent materials has become a research hotspot. Luminescent materials can be divided into fluorescence (FL) and afterglow materials according to the transition pathway (Gao et al., 2021). Owing to the limitation of exciton statistics, it is difficult to further improve the quantum utilization efficiency of FL materials, and the luminescent lifetime is short. Afterglow materials can release the stored excitation energy and continue to maintain luminescence after the excitation of external energy is removed, so afterglow materials can overcome the inherent defects of the FL materials.

Afterglow materials date back to the early seventeenth century and they are divided into inorganic and organic systems (Yen et al., 2007). Inorganic afterglow materials, which have been commercialized, involving rare earth or transition metal ions doped in the matrix, such as  $\text{Eu}^{2+}$ ,  $\text{Dy}^{3+}$  and  $\text{Mn}^{2+}$  (Matsuzawa et al., 1996). However, they have high cost because of the doping of rare earth or transition metal ions and high-consumption preparation conditions, the tedious processing technology, and biological toxicity, limiting their practical applications. Organic afterglow materials, with the merits of low cost, easy preparation and good biocompatibility, have been gradually brought into public view. They are mainly divided into room temperature phosphorescence (RTP) and delayed fluorescence (DF) materials. As the second generation of organic light-emitting materials (Tao et al., 2014), the luminescent lifetime and quantum efficiency of RTP materials are improved effectively owing to the intersystem crossing (ISC) process. However, RTP materials are confined to noble metal such as platinum and iridium because of the exciton quenching effect caused by weak spin-orbit coupling, which results in relative high cost. The DF materials can effectively combine the low cost of FL and high efficiency of RTP, providing a perspective for novel luminescent materials. Owing to the advantages of diverse structures, simple synthesis, easy purification and high luminescent efficiency, pure organic and metal-organic complexes are dominant in the research of organic DF materials. However, organic DF materials still have many shortcomings that limit their further development. For example, the DF lifetime of organic molecules is relatively short because their triplet excitons are easily

<sup>1</sup>Key Laboratory of Interface Science and Engineering in Advanced Materials, Ministry of Education, Taiyuan University of Technology, Taiyuan 030024, China

<sup>2</sup>College of Materials Science and Engineering, Taiyuan University of Technology, Taiyuan 030024, China

<sup>3</sup>Shanxi-Zheda Institute of Advanced Materials and Chemical Engineering, Taiyuan 030032, China

\*Correspondence: [yzytyt@126.com](mailto:yzytyt@126.com) (Y.Y.), [yanlingpeng@tyut.edu.cn](mailto:yanlingpeng@tyut.edu.cn) (L.Y.)

<https://doi.org/10.1016/j.isci.2022.104884>



deactivated by non-radiative process from the active excited triplets (Yuan et al., 2015), and the organic solvents used in the preparation are harmful to environment. Metal complexes are relatively expensive and toxic. Therefore, it is necessary to explore a kind of novel DF materials with stable luminescence, environmental friendliness, and low cost.

Carbon dots (CDs) have become a new generation of carbon nanoluminescent materials following fullerene, carbon nanotubes, and graphene, because of their excellent photostability, low toxicity, low cost, tunable photoluminescence, and so on. They have demonstrated considerable application prospects in light-emitting diodes, solar cells, biological imaging, sensing, detection, medical treatment, UV-blocking and other fields (Zhang et al., 2016a; Zhang et al., 2016b; Xu et al., 2018a; Xu et al., 2018b; Wang et al., 2018a; Ding et al., 2019; Yuan et al., 2019; Zhao et al., 2021; Zhao et al., 2020b; Atabaev, 2018; Zhang et al., 2022; Ali et al., 2020; Ghosh et al., 2021a; Ghosh et al., 2021b; Kailasa and Koduru, 2022; Feng et al., 2017; Ashrafzadeh et al., 2020; Dong et al., 2019; Kousheh et al., 2020; Wang et al., 2021a). Since the discovery of CDs in 2004 (Xu et al., 2004), the research on CDs has mainly focused on their synthesis and fluorescence performance regulation (Ju et al., 2017; Qu and Sun, 2020; Wang et al., 2018b). In general, the methods to prepare CDs can be divided into "top-down" and "bottom-up" approaches. The "top-down" method is the way to directly obtain CDs from large-sized carbon source (such as graphite, graphene, carbon fiber, carbon nanotubes) by decomposition and exfoliation process. The CDs prepared by "top-down" approach usually exhibit higher crystallization (Zhao et al., 2021) whereas the "bottom-up" method is the way to prepare CDs from organic small molecules by carbonization and polymerization reaction. The CDs prepared by "bottom-up" generally possess the controlled optical behavior because of controllable size and heteroelement doping (Zhang et al., 2016). Lin et al. (2012) synthesized CDs by doping  $Pb^{2+}$  ions with stable FL and RTP for the first time. By hydrothermal treatment and annealing of graphene oxide sheets under alkaline conditions, Tetsuka, et al. (2012) obtained amino-functionalized graphene quantum dots with the sub-second DF property. Later, the afterglow CDs began to attract the attention of researchers, and the RTP and DF CDs were successively reported (Dong et al., 2015; Jiang et al., 2016; Kang et al., 2021). The afterglow performance of CDs exhibits their potential to be promising candidates for DF materials as a novel type of green materials. To date, CDs-based DF materials can be constructed by matrix-assisted or self-protective method. By providing a rigid protection of matrix (such as silica, zeolite, boric acid) or the polymer chain structure, the excited triplet state can be stabilized, which provides more possibilities for the generation of DF (Han et al., 2021; Liu et al., 2017; Xu et al., 2020a). The key factor of the CDs-based DF materials is the regulation of the energy difference between the excited singlet state and excited triplet state ( $\Delta E_{ST}$ ), a relative smaller  $\Delta E_{ST}$  is more conducive to the reverse intersystem crossing (RISC) for DF generation. Although the CDs-based DF materials have made some progress, their luminescence mechanism and controllable synthesis still need to be explored. In this review, the DF mechanism, structural control strategy, and their application progress in temperature sensing, anti-counterfeiting icons, information encryption and other fields of CDs-based DF materials are summarized. Finally, the future development of CDs-based DF materials is prospected.

## DF MECHANISM OF CDS-BASED MATERIALS

DF belongs to a kind behavior of photoluminescence, which refers to the process of electron transition from ground state ( $S_0$ ) to unstable excited state ( $S_m, T_m$ ) after light excitation and then back to  $S_0$  state after radiation transition. Based on the Pauli incompatibility principle, the excited state can be classified as the excited singlet ( $S_1, S_2, \dots, S_n$ ) and the triplet ( $T_1, T_2, \dots, T_n$ ) states according to the spin multiplicity (Xiao and Zhang, 2020). The spin pairing corresponds to the excited state as the singlet state. After the electron spin direction is reversed, the spin is parallel, the spin multiplicity changes, and the excited state is named as the triplet state. As shown in Figure 1, FL is formed by electrons transition from the excited singlet state to the ground state. Phosphorescence is generated by electrons at the excited triplet state transition to the ground state. DF is formed when electrons transfer back to the excited singlet state from the triplet state and then return to ground state radiatively.

As an organic/inorganic hybrid system, the DF mechanism of CDs-based DF materials can be explained from inorganic and organic systems. There are two origins for CDs-based DF materials; one is related to the excited triplet state of organic matter and the other to the defect energy level of inorganic matter. The energy level state plays a decisive role in CDs-based DF materials (Deng et al., 2013; Dias et al., 2017; Xu et al., 2016). The DF mechanism of CDs-based composites can be divided into four mechanisms according to the energy level state (Figure 1): thermally activated delayed fluorescence (TADF),

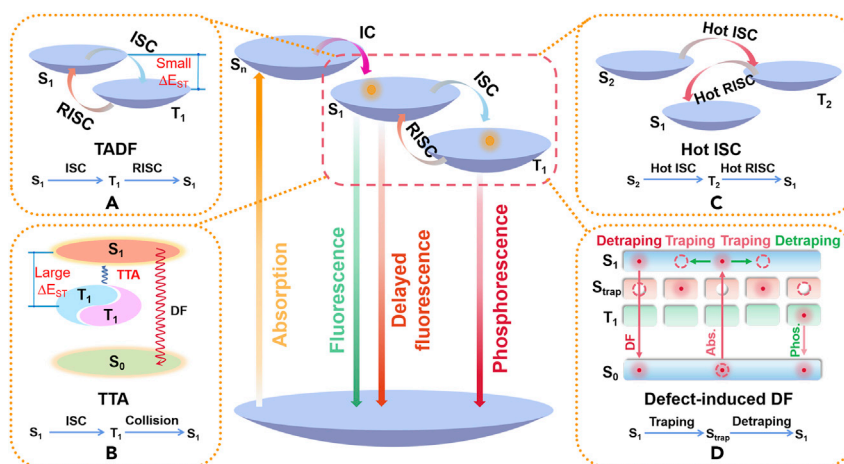


**Figure 1. Mechanisms of CDs-based DF materials**

- (A) TADF light-emitting mechanism.  
 (B) TTA light-emitting mechanism.  
 (C) Hot ISC DF light-emitting mechanism.  
 (D) Defect-induced DF light-emitting mechanism.

triplet-triplet annihilation (TTA), “hot excitons” intersystem crossing (Hot ISC), and defect-induced delayed fluorescence.

### Thermally activated delayed fluorescence (TADF)

TADF involves an RISC process, that is, the electrons transition from the triplet excited state to the singlet excited state and then back to the ground state ( $S_0$ ). When the radiative transition rate between the lowest excited triplet state ( $T_1$ ) and the lowest excited singlet state ( $S_1$ ) is greater than the non-radiative transition rate of the triplet excitons, TADF is generated. The electron transition process is shown in Figure 1A. After absorbing the light energy, the electrons transition from  $S_0$  to  $S_1$  and then to  $T_1$  through ISC. Subsequently, they return back to  $S_1$  through RISC, and transition radiatively to  $S_0$  ( $S_0 \rightarrow S_1 \rightarrow T_1 \rightarrow S_1 \rightarrow S_0$ ). According to the spin (exciton) statistics, the number ratio of the excited singlet to the triplet excitons is 1:3 (Baldo et al., 1999). Therefore, the internal quantum efficiency (IQE) of FL is up to 25%, and the remaining 75% excitons accumulate in excited triplet after ISC, which indicates that TADF can reach 100% IQE theoretically. According to Hund’s rule, the spin paralleling is more stable than spin pairing, and the excited triplet state energy is lower than the corresponding singlet state. Therefore, RISC needs external energy (usually thermal energy) activation, which requires TADF to meet sufficiently small  $\Delta E_{ST}$  to absorb the thermal activation energy to promote the efficient RISC. At the same time, it is necessary to suppress the non-radiative deactivation of excited triplet state to promote the occurrence of RISC process.

Because TADF belongs to the thermal activation process, TADF luminescence intensity enhances with the increase of temperature in a certain temperature range (Figures 2A, 2B, and 2C), which makes TADF material stand out in higher temperature environment. Based on the high IQE, TADF materials have become the representative materials of the third generation OLEDs in organic luminescence materials. In recent years, it has been found that CDs-based composites also have TADF properties (Liu et al., 2017; Xu et al., 2020a; Sun et al., 2020a; Park et al., 2020; Liu et al., 2020; He et al., 2020; Mo et al., 2021; Liu et al., 2019; Zhang et al., 2020a; He et al., 2021; He et al., 2018; Jiang et al., 2017; Hou et al., 2015), which opens up a novel pathway for developing of advanced TADF materials.

### Triplet-triplet annihilation (TTA)

The TTA process refers to the transformation from two excited triplet excitons to one excited singlet exciton after collision and annihilation. The radiative transition of this excited singlet exciton to the ground state generates DF (Figure 1B) (Chiang et al., 2013). Compared with TADF, large  $\Delta E_{ST}$  is more conducive to the accumulation of triplet excitons to promote TTA. This mechanism is also reflected in CDs-based DF composites. Han et al. (2021) obtained TPA-CDs/Si solution by hydrothermal method in alkaline

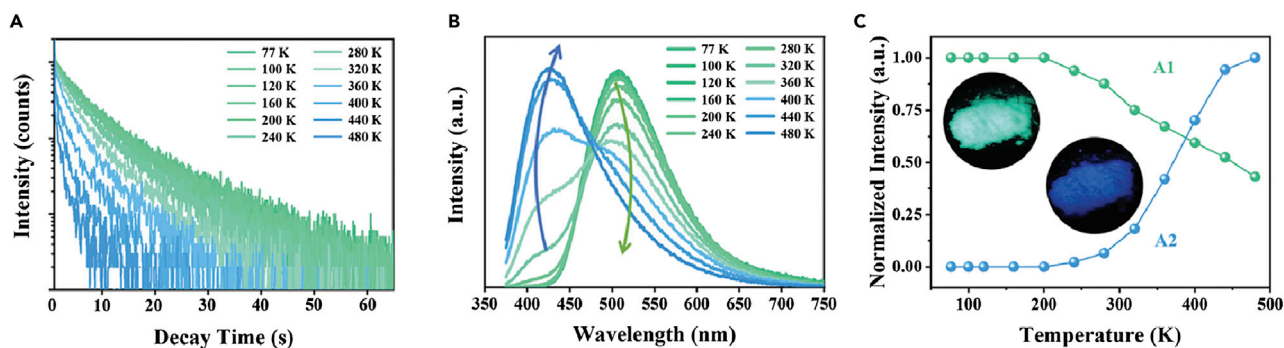


**Figure 2. CD-based TADF materials**

(A) Temperature-dependent afterglow decay curves of CDs@SiO<sub>2</sub> TADF materials with 365 nm excitation.

(B) Temperature-dependent afterglow emission spectra of CDs@SiO<sub>2</sub> under excitation at 365 nm.

(C) Line chart of temperature-dependent RTP (A1) and TADF (A2) intensities, and photographs of RTP and TADF (inset). Reproduced with the permission from (Sun et al., 2020a). Copyright 2019 Royal Society of Chemistry.

environment with terephthalic acid as carbon source and colloidal SiO<sub>2</sub> as silicon source, and then synthesized TPA-CDs/Si powder after calcination. This composite material has a water-triggered tuning responsive afterglow property (Figures 3A and 3B). This afterglow includes the mixed emission of DF and RTP at room temperature. Because this DF property does not have the enhanced characteristics with increasing temperature (Figure 3C), not belong to TADF or defect-induced DF, in view of its  $\Delta E_{ST}$  does not change apparently with the excitation wavelength (0.041 eV at 254 nm, 0.045 eV at 365 nm), its DF generated from TTA mechanism (Salla et al., 2019). In this work, TPA-CDs/Si are quasi-spherical nanoparticles with sp<sup>2</sup> carbon skeleton as the core. The Si–C covalent bond formed by Si as the doping element is the DF source of TPA-CDs/Si, and the intramolecular hydrogen bond is their RTP source. After adding a certain amount of water, the DF strength of TPA-CDs/Si decreases rapidly until it disappears, while RTP gradually becomes dominant, with the afterglow color changing from blue to green. This is because the formation of hydrogen bond network between water and TPA-CDs/Si is beneficial to RTP emission. When the amount of water exceeds a certain limit, RTP intensity begins to decrease with the enhancement of non-radiative vibration relaxation. Surprisingly, the DF of TPA-CDs/Si recover after the water is removed by heating. This method realizes color-tunable and reversible afterglow by adding water to build hydrogen bond networks or heating to remove water for destroying hydrogen bonds, which can be used in multi-level encryption and decryption fields (Han et al., 2021).

In organic DF materials, the maximum IQE of TTA mechanism only reach 62.5% because of the limitation of excited triplet and singlet energy levels (Godumala et al., 2016). Therefore, the exciton utilization rate of DF by TTA mechanism is limited, which restricts the practical application of TTA materials.

### Hot intersystem crossing

TADF and TTA processes are described as the cold excitons process (Hu et al., 2015). Hot excitons refer to the excitons that transition to a higher excited state (i.e.,  $S_n$ ,  $T_m$ ) after light excitation (Yao et al., 2014). The transformation from the excited singlet hot excitons to the excited triplet hot excitons is defined as hot ISC process (Figure 1C). Accordingly, the transformation from the excited triplet hot excitons to the excited singlet hot excitons is hot RISC process (Figure 1C). The radiative transition between the excited triplet excitons and excited singlet excitons at higher energy levels is better than the vibrational relaxation of their own transition to low energy levels, which is beneficial to the hot ISC process. According to Kasha's rule (Xu et al., 2019), the internal conversion rate ( $k_{IC}$ ) between the excited states with same spin multiplicity is often higher than the ISC rate ( $k_{ISC}$ ). Therefore, the prerequisite for realizing the RISC of triplet hot excitons to transform into singlet excitons is that the energy difference between the higher excited triplet state ( $T_m$ ) and the  $T_1$  state is large enough. Thus, the accumulation of triplet hot excitons in triplet state is greatly reduced, which results in the reduction of the probability for TTA and singlet-triplet state quenching (STA). Finally, DF is generated through RISC.

Lin et al. (2019) synthesized the nitrogen-doped CDs-based DF materials (NCD1-C) with excitation dependent afterglow. The NCD1-C materials present DF under 254 nm excitation and RTP under 365 nm

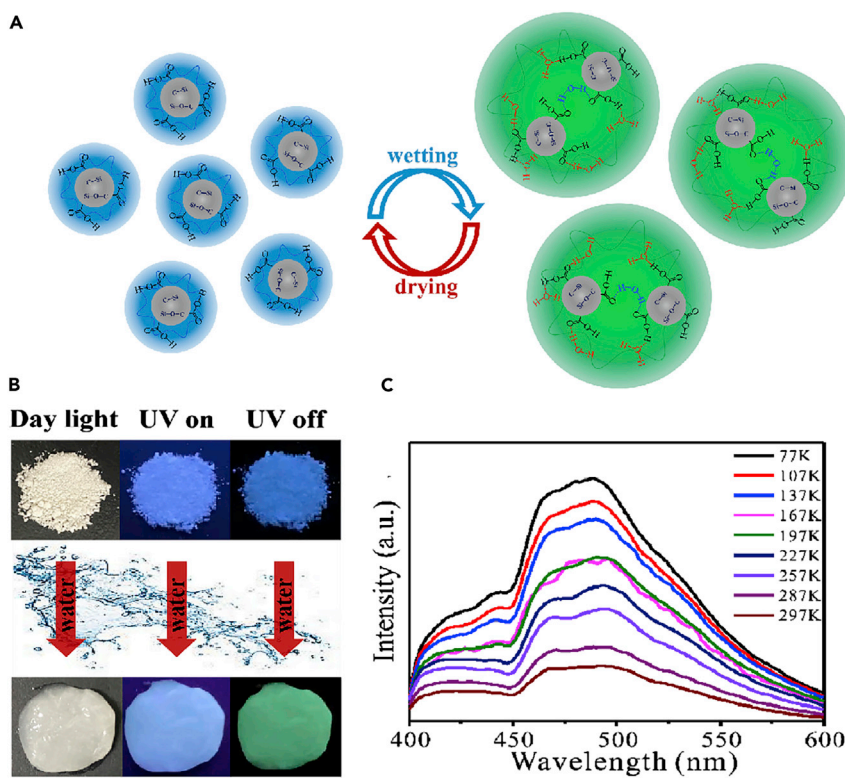


**Figure 3. CDs-based TTA materials**

(A) Schematic illustration of mutual transformation process of TPA-CDs/Si and TPA-CDs/Si@H<sub>2</sub>O.

(B) Photographs of TPA-CDs/Si before and after adding water under sunlight, before and after turning off 254 nm UV light.

(C) Afterglow emission spectra of TPA-CDs/Si under 254 nm UV irradiation at different temperatures. Reproduced with the permission from (Han et al., 2021). Copyright 2021 Elsevier.

excitation. Under 365 nm excitation, their TADF property is triggered by increasing temperature. As shown in Figure 4A, under high energy of the short-wavelength excitation (254 nm), the electrons transfer to the higher excited singlet state ( $S_2$ ), and then to the higher excited triplet state ( $T_2$ ) through hot ISC. Because the energy difference between  $T_2$  state and the  $T_1$  state is greater than that between  $T_2$  state and the  $S_1$  state, the triplet hot excitons transition to  $S_1$  state through hot RISC process and then return to the  $S_0$  state to generate DF ( $S_0 \rightarrow S_2 \rightarrow T_2 \rightarrow S_1 \rightarrow S_0$ ). When the electrons transition to the  $S_1$  state and then come to  $T_1$  state by ISC under long wavelength (365 nm) excitation, there are two kinds of transition forms: one is the transition back to  $S_0$  state radiatively to generate RTP ( $S_0 \rightarrow S_1 \rightarrow T_1 \rightarrow S_0$ ), another is the transition to the  $S_1$  state through RISC, and then back to  $S_0$  state to produce TADF ( $S_0 \rightarrow S_1 \rightarrow T_1 \rightarrow S_1 \rightarrow S_0$ ) when the temperature increases.

Deng et al. (2019) not only studied the excitation-dependent afterglow properties of CDs@clay composites, but also illustrated that the DF lifetime of hot exciton process was longer than that of the RTP of cold exciton process by comparing the afterglow lifetimes at two excitation wavelengths. Their research shows that blue DF is formed by hot exciton process under short wavelength (254 nm) excitation and DF intensity decreases with the increase of temperature (Figure 4B). Under the excitation of long wavelength (302 nm), the green afterglow generated by cold exciton process is dominated by RTP, and TADF gradually has more advantages with the increase of temperature (Figure 4C). The electronic transition path of CDs@clay composite after excitation is consistent with the Figure 4A. At room temperature, the average afterglow lifetime (1.050 s) excited at 254 nm is obviously higher than that (0.608 s) at 365 nm, which is because the DF with hot exciton process involves two spin-forbidden transitions.

Hot excitons DF materials not only have higher luminescence efficiency than TADF materials, but also effectively solve the serious roll-off problem in electroluminescent devices with TTA materials. Therefore, they have a potential application prospect in organic electroluminescent devices. CDs-based hot exciton DF



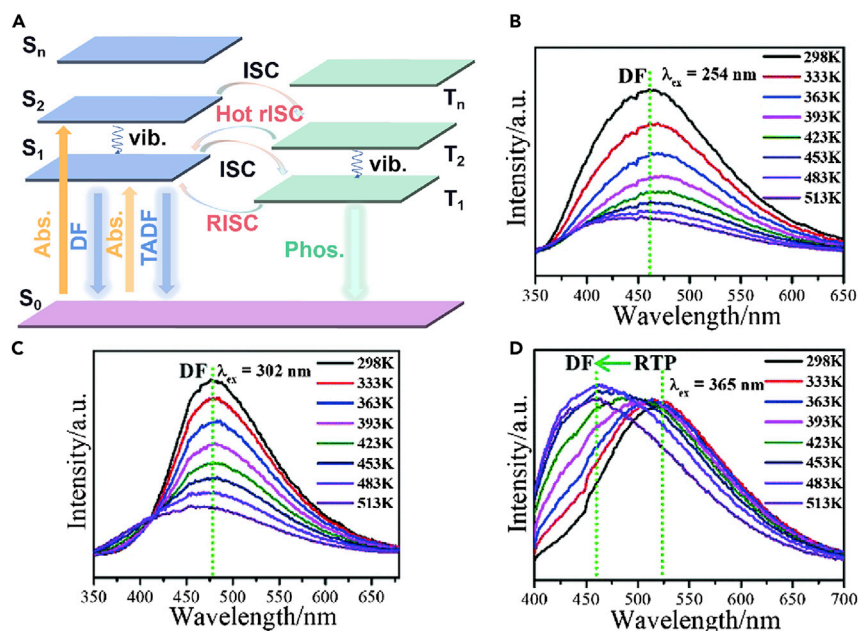


**Figure 4. CDs-based Hot ISC materials**

(A) Hot ISC DF light-emitting mechanism. Afterglow emission spectra of CDs@clay (B) at different temperatures under 254 nm excitation, (C) at different temperatures under 302 nm excitation, and (D) under different excitation wavelengths. Reproduced with the permission from (Deng et al., 2019). Copyright 2019 Royal Society of Chemistry.

composites can achieve the applications of multi-level anti-counterfeiting and encryption because of the different conversion modes of triplet excitons under different excitation wavelengths. However, high energy input is essential to generate DF behavior, which limits their applications.

### Defect-induced delayed fluorescence

The afterglow properties of inorganic long afterglow materials are related to their luminescent and defect centers. Defects can capture some stimulated electrons and re-release them under certain environmental factors. The luminescent process by releasing electrons through thermal disturbance is usually called thermoluminescence (Bos, 2017). CDs-based DF materials can also be obtained by using trapping-detrapping mechanism to stabilize triplet excitons (Xu et al., 2020b). As shown in Figure 5A, the CDs-SiO<sub>2</sub> composites synthesized by He et al. (2020) exhibit phosphorescence enhancement and DF characteristics in solid and liquid phases by introducing inorganic SiO<sub>2</sub> as matrix. The electron trap center of inorganic SiO<sub>2</sub> matrix is the key to enhance phosphorescence and DF. The electrons in S<sub>0</sub> state are excited by light to become excited electrons. In the process of returning to S<sub>0</sub> state, some electrons are captured by the electron trap state (S<sub>trap</sub>) located between S<sub>1</sub> and T<sub>1</sub> state. The energy gap between S<sub>trap</sub> state and S<sub>1</sub> state is 0.297 eV whereas the energy gap between S<sub>trap</sub> state and T<sub>1</sub> state is 0.271 eV. Therefore, there are two transition paths for the released electrons to return to S<sub>0</sub> state (Figure 5C). Some electrons in the trap state will detrapp to T<sub>1</sub> or S<sub>1</sub> state and then return to S<sub>0</sub> state as the form of phosphorescence (S<sub>0</sub> → S<sub>1</sub> → S<sub>trap</sub> → T<sub>1</sub> → S<sub>0</sub>) or DF (S<sub>0</sub> → S<sub>1</sub> → S<sub>trap</sub> → S<sub>1</sub> → S<sub>0</sub>), respectively. The mechanism of inorganic afterglow materials is usually explained through the distribution of internal traps by thermoluminescence spectroscopy (Zhang et al., 2021). As shown in Figure 5B, the thermoluminescence spectroscopy (Figure 5B) was also used for the first time to study the CDs-based DF composites, proving that the electronic defects of inorganic SiO<sub>2</sub> can act on the energy level state of CDs, thereby regulating the phosphorescence and TADF behaviors.

In summary, the different conversion modes between the triplet excitons and singlet excitons can generate different DF behavior. The triplet excitons in TADF are converted into the singlet excitons by RISC under thermal activation. TTA mechanism needs the accumulation of triplet excitons, Hot ISC and hot RISC depend on the excitation of specific energy. Defect-induced DF requires additional electronic defects and thermal activation.  $\Delta E_{ST}$  is of vital importance to the conversion between triplet excitons and singlet excitons. Small  $\Delta E_{ST}$  can facilitate ISC process and offer more possibilities to harvest triplet excitons

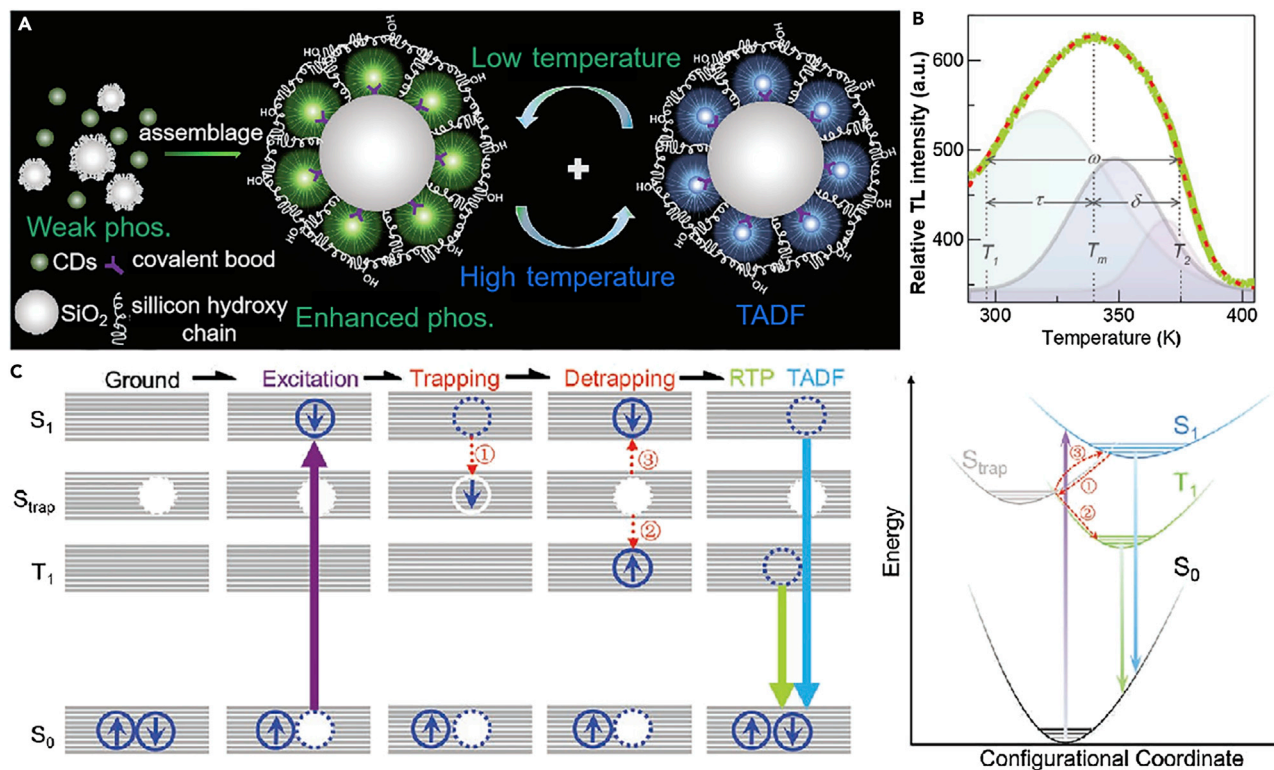


**Figure 5. CDs-based defect-induced DF materials**

(A) The schematic illustration of CDs anchored onto SiO<sub>2</sub> for phosphorescence enhancement and TADF nascence, and the conversion between them with the change of temperature.

(B) Thermoluminescence spectra of CDs-SiO<sub>2</sub> powder (green solid line: recorded data; colored areas: peak fitting; red dashed line: accumulated fitting).

(C) Defect-mediated thermoluminescence (Jablonski diagram and configuration coordinate curves). Reproduced with the permission from (He et al., 2020). Copyright 2020 Wiley-VCH.

more efficiently, thus the DF process can be achieved more easily. For CDs-based DF materials, the realization of DF is closely related to their excited triplet state, in which the stable excited triplet state and small  $\Delta E_{ST}$  are the key factors. The stabilizing excited triplet state and reducing  $\Delta E_{ST}$  can provide a theoretical foundation for the structural and performance regulation of CDs-based DF materials.

### STRUCTURAL REGULATION STRATEGY OF CDS-BASED DF MATERIALS

Based on the DF mechanism in the above-mentioned CDs-based DF materials, inhibiting the quenching of the excited triplet state and reducing the  $\Delta E_{ST}$  are two key factors that must be considered in the synthesis of CDs-based DF materials. Therefore, it is necessary to regulate the structure and properties of CDs-based DF materials by stabilizing the excited triplet state and controlling the energy difference.

#### Excited triplet state stabilization

At present, there are two main synthesis methods to stabilize triplet state: matrix-assisted and self-protective method (Sun et al., 2020b; Li et al., 2019a; Chen et al., 2017; Jiang et al., 2020b). Matrix-assisted method is that CDs are embedded into different matrices to form a rigid structure by the interaction between matrix and CDs for suppressing the non-radiative relaxation by rotation and vibration. The self-protective method is that the polymer-like structures of carbonized polymer dots (CPDs) limit molecular motion to stabilize the excited triplet state.

##### Matrix-assisted method

The luminescent center is fixed by covalent bond or hydrogen bond between matrix and CDs, which can improve the rigidity of molecular structure and inhibit the quenching effect of dissolved oxygen and water on the excited triplet state, so as to effectively stabilize the excited triplet state to generate DF. The

different kinds of matrices have been used to stabilize the excited triplet state. As shown in Table 1, the CDs-based DF composites synthesized by matrix-assisted method in recent years are summarized. The preparation of CDs-based DF composites can be classified into two-step and *in-situ* method according to the process steps. The two-step method is simple in principle and rich in matrix types, including inorganic matrices (such as SiO<sub>2</sub>, zeolite, and boric acid), organic matrices (such as polyvinyl alcohol (PVA) and polyurethane (PU)). The *in-situ* method simplifies the synthesis process, but matrix is limited. At present, zeolites-based inorganic matrix is mainly used for *in-situ* synthesis of CDs-based DF composites.

### Inorganic matrices

**SiO<sub>2</sub>.** Nanosized SiO<sub>2</sub>, as a kind of ordered mesoporous materials, can provide rigid nano-space for luminescent particles (CDs, perovskite quantum dots, etc.). They can be used as a suitable matrix for long-lifetime emission materials in fields of biological imaging and sensors (Joseph and Anappara, 2017; Li et al., 2019b). In the SiO<sub>2</sub> matrix system, CDs can be effectively fixed by the hydrogen bonds or covalent bonds between the surface functional groups of CDs and SiO<sub>2</sub>. SiO<sub>2</sub> with silicon-oxygen tetrahedron structure can inhibit the vibration and rotation of luminescent center of CDs to stabilize the excited triplet state, and nanosized SiO<sub>2</sub> particles can also prevent the diffusion of oxygen, offering higher stability and longer lifetime.

Jiang et al. (2017) firstly synthesized TADF-dominated liquid phase long-lived CDs matrix composites (*m*-CDs@nSiO<sub>2</sub>) at room temperature using *m*-phenylenediamine as carbon source and nSiO<sub>2</sub> as matrix. The formation of Si–C and Si–N covalent bonds in *m*-CDs@nSiO<sub>2</sub> is the key factor that can produce stable afterglow in the liquid phase. And the unsaturated C=C bond on the surface of *m*-CDs can consume dissolved oxygen, which also provides a practicable approach to inhibit the quenching effect of oxygen on the triplet state. The sol-gel method can prepare a gel with certain spatial structure, and the nanoparticles can be obtained after gel heat treatment (Jiang et al., 2019). Sun et al. (2020a) embedded CDs in the nano-silica gel network by this method. After calcination, the CDs-based composite (CDs@SiO<sub>2</sub>), with temperature-responsive conversion of RTP and TADF, was prepared. As shown in Figure 6A, the Si–O network plays an essential role in afterglow emission of CDs@SiO<sub>2</sub>, the formation of hydrogen and covalent bonds (Si–O–C, Si–C) enhances the structural rigidity, and the nano-space confinement effect makes the excited triplet state more stable. Therefore, under the comprehensive effects of rigid Si–O network structure protection, strong covalent bond assistance and effective spatial constraint, a more stable excited triplet state T<sub>1</sub>\* is generated, which makes CDs@SiO<sub>2</sub> display ultra-long stable phosphorescence at room temperature. This triplet emission is attributed to the n-π\* transition of C=O. Because of the relatively large ΔE<sub>ST</sub> (0.53 eV), it is difficult to active effective RISC at room temperature, CDs@SiO<sub>2</sub> only present TADF at higher temperature (An et al., 2015; Tang et al., 2019).

Liu et al. (2020) used modified Stober method to synthesize long-lifetime TADF material CD@SiO<sub>2</sub> at room temperature by embedding CDs into nano-silica microspheres (Figure 6B). The Si–O–C covalent bonds restrict the vibration and rotation of CDs luminescence centers (C=O, C=N) and suppresses the non-radiative energy dissipation, thus stabilizing the excited state. Recently, Mo, et al. (2021) realized the long-lived TADF excited by visible light in the liquid phase using amorphous silicon nanoparticles as matrix to encapsulate fluorine and nitrogen co-doped CDs. The strong electronegativity of fluorine atoms can reduce the energy difference between the highest occupied molecular orbital (HOMO) and lowest unoccupied molecular orbital (LUMO), so as to reduce the excitation energy and realize visible light excitation. In Figure 6C, amorphous SiO<sub>2</sub> can protect the excited triplet state by forming hydrogen bond network, and the silanol groups on SiO<sub>2</sub> surface can endow F, NCDs@SiO<sub>2</sub> composites with good hydrophilicity, achieving higher efficiency of liquid phase DF.

**Zeolite.** Zeolite, as an inorganic porous material, has become one of the ideal materials for loading and packaging metal nanoparticles and luminescent quantum dots due to its three-dimensional ordered structure and strong thermal stability (Li et al., 2015; Wang et al., 2012). In the zeolite matrix system, its interrupted nanospace can restrict the intramolecular vibration and rotation. Moreover, the hydrogen bonds, which are formed by the dangling OH groups of the interrupted nanospace and surface groups (C=N and C=O) of CDs, can effectively inhibit the non-radiative relaxation. The 3D framework of zeolite can also hinder the collisions between oxygen and the surface groups of CDs, which plays a role in stabilizing the excited triplet states to generate ultra-long and stable DF at room temperature (Liu et al., 2017).



**Table 1. Matrix assisted CDs-based DF composites**

Method	Matrix	Precursor	Afterglow mode (298 K)	$\Delta E_{ST}/eV$	Afterglow lifetime ( $\tau$ )/ms (298 K)	QY (%)	Remarks	Ref.	
Two-step	SiO <sub>2</sub>	mPDs	TADF + RTP	0.290 (Ex. = 365 nm)	703 (Ex. = 365 nm)	NA	m-CDs@nSiO <sub>2</sub>	(Jiang et al., 2017)	
		PVA, EDA	TADF + RTP	0.568 ( $\Delta E_{ST}$ trap = 0.297; $\Delta E_{T}$ trapT1 = 0.271) (Ex. = 340 nm)	1760 (Ex. = 340 nm)	35	CDs-SiO <sub>2</sub>	(He et al., 2020)	
	BA	2,4-Difluorobenzoic acid, Glycine	TADF + RTP	0.32 (Ex. = 460 nm)	$\tau$ RTP: 610, $\tau$ TADF: 270 (Ex. = 460 nm)	58.8	F, NCDs@SiO <sub>2</sub>	(Mo et al., 2021)	
		RhB	TADF + RTP	NA	447.96 (Ex. = 420 nm)	38.07	G-CDs/B <sub>2</sub> O <sub>3</sub>	(Xu et al., 2020a)	
		GNPs	TADF	0.186 Ex. = 325 nm	135 Ex. = 325 nm	1.39	GOQD-30@BNO;	(Park et al., 2020)	
	PVA	PVA, EDA			0.156	147	0.90	GOQD-40@BNO;	
					0.123	125	0.86	GOQD-60@BNO	
				RTP + TADF	0.0367 (Ex. = 360 nm)	$\tau$ TADF: 1610; $\tau$ RTP: 0.00681 (Ex. = 360 nm)	22.57	CDs/PVA nanofiber	(He et al., 2018)
	Urea	Citric acid, Urea, 4-aminobenzoic acid	DF	NA	$\tau$ Core-state: 206.1; $\tau$ N-state: 247.4	NA	CD2-H/PVA	(Zhai et al., 2021)	
		Folic acid, Ethanol	Hot ISCDF	NA	1113.27, 534.52 (Ex. = 254 nm, 365 nm)	13.9 (Prepared at pH = 7)		(Lin et al., 2019)	
oPD		RTP + TADF	0.481 (Ex. = 365 nm)	$\tau$ TADF: 220.74; $\tau$ RTP: 12.29 (Ex. = 365 nm)	3 (Ratio of o-CDs to urea is 0.05%)	o-CDs@CA	(Wang et al., 2021b)		
In situ	Zeolite	TEA	TADF	0.22 (Ex. = 370 nm)	350 (Ex. = 370 nm)	15.33	CDs@AlPO-5	(Liu et al., 2017)	
		Valine, EDA	RTP + TADF	0.35 (Ex. = 400 nm)	$\tau$ RTP: 1700; $\tau$ DF: 2100 (Ex. = 400 nm)	90.4	CDs@AlPO-5 composite	(Zhang et al., 2020b)	
	Layered clay	Pyridine-2,6-dicarboxylic acid		0.095(Ex. = 254 nm)	1050 (Ex. = 254 nm)	NA	CDs@clay	(Deng et al., 2019)	
				0.27 (Ex. = 302 nm)	1020 (Ex. = 302 nm)				
				0.62 (Ex. = 365 nm)	608 (Ex. = 365 nm)				

NA: Not available;  $\Delta E_{ST}$ : The difference between excites singlet and triplet state; QY: Absolute quantum yield; TADF: Thermally activated delayed fluorescence; RTP: Room temperature phosphorescence; DF: Delayed fluorescence; Hot ISC: Hot excitons intersystem crossing; mPDs: m-phenylene diamine; TTDDA: 4,7,10-trioxa-1,13-tridecanediamine; RhB: Rhodamine B; GNPs: Graphite nanoparticles; IPDI: Isophorone diisocyanate; PVA: Polyvinyl alcohol; EDA: Ethylenediamine; oPD: o-phenylenediamine; TEA: Triethylamine.



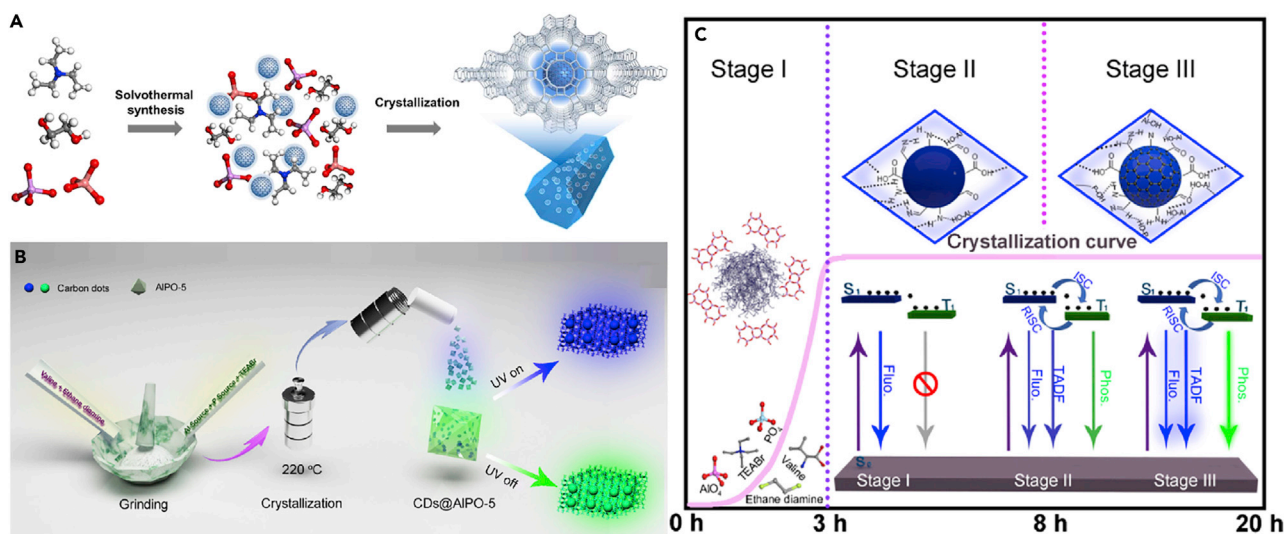


**Figure 7. Zeolite-assisted CDs-based DF composites**

(A) Proposed in situ formation process of photoluminescent CDs@AIPO-5 composite. Reproduced with the permission from (Liu et al., 2017). Copyright 2017 Science AAS.

(B) Schematic representation of confinement synthesis of CDs in AIPO-5 zeolite.

(C) CDs@AIPO-5 formed with varying crystallization time and proposed crystallization curve of the CDs@AIPO-5 composite. Reproduced with the permission from (Zhang et al., 2020b). Copyright 2020 Chinese Chemical Society.

can induce the quenching of DF, which limits the application of BA-assisted DF materials in liquid environment such as biological probes.

Xu et al. (2020a) synthesized the visible-light-excited afterglow composite (CDs/B<sub>2</sub>O<sub>3</sub>) with main emission of TADF at room temperature by embedding green CDs into the glassy B<sub>2</sub>O<sub>3</sub> matrix. The key factors for afterglow of CDs/B<sub>2</sub>O<sub>3</sub> composite are glassy B<sub>2</sub>O<sub>3</sub> matrix and the B atoms with empty p-orbital. Green CDs dispersed in the glassy B<sub>2</sub>O<sub>3</sub> matrix can effectively inhibit the aggregation fluorescence quenching, and protect the triplet excitons from quenching. The boron atoms with empty p-orbital can attract  $\pi$  electron to produce a p- $\pi$  conjugate system, which reduces LUMO energy level, decreasing the  $\Delta E_{ST}$  and making visible-light excitation possible. As shown in Figure 8A, Park, et al. (2020) used BNO matrix from BA to stabilize the excited triplet state of graphene quantum dots (GQDs) and achieve TADF. He et al. (2021) prepared a series of visible-light-excited afterglow CDs/B<sub>2</sub>O<sub>3</sub> composites as Xu et al. (2020a), in which the color of composites was regulated by changing CDs precursor (Figure 8B).

**Layered clay.** In addition to the above-mentioned inorganic matrices, the layered clay synthesized by layered silicate also can act as the matrix of CDs-based DF materials. Deng et al. (2019) achieved CDs@clay composites with triple-emission (FL, RTP, DF) and tunable afterglow characteristics by covalently confining CDs on the clay layer through calcination. The triple-emission of the composites mainly is generated by the n- $\pi^*$  transition of C=O with a conjugated aromatic group and covalent bonds between CDs and clay sheets. The n- $\pi^*$  transition of C=O with a conjugated aromatic group is the main origin of FL and afterglow, which is beneficial to the ISC process. And the formation of covalent bonds can fix the luminescence center to stabilize the excited triplet state (Katsurada et al., 2015). The afterglow properties of the composites depend on whether the electrons are excited to the S<sub>2</sub> state or S<sub>1</sub> state. The electrons are excited to S<sub>2</sub> state at short-wavelength excitation, the ISC between the S<sub>2</sub> and T<sub>2</sub> state and the RISC between T<sub>2</sub> and S<sub>1</sub> state are easy to happen, resulting in the dominated role of DF at room temperature. However, the electrons are excited to S<sub>1</sub> state at long-wavelength excitation, the ISC between the S<sub>2</sub> and T<sub>2</sub> state starts-up, inducing the leading role of RTP. Moreover, with the increase of temperature, the RISC between T<sub>1</sub> and S<sub>1</sub> state gradually enhances, thus the RTP decreases and TADF becomes dominant.

**Organic matrices.** The incorporation of CDs into organic matrix is a common method to realize the phosphorescence emission of CDs. The excited triplet state can be stabilized by hydrogen bonding between organic matrix and CDs, which is also conventional in CDs-based DF composites.

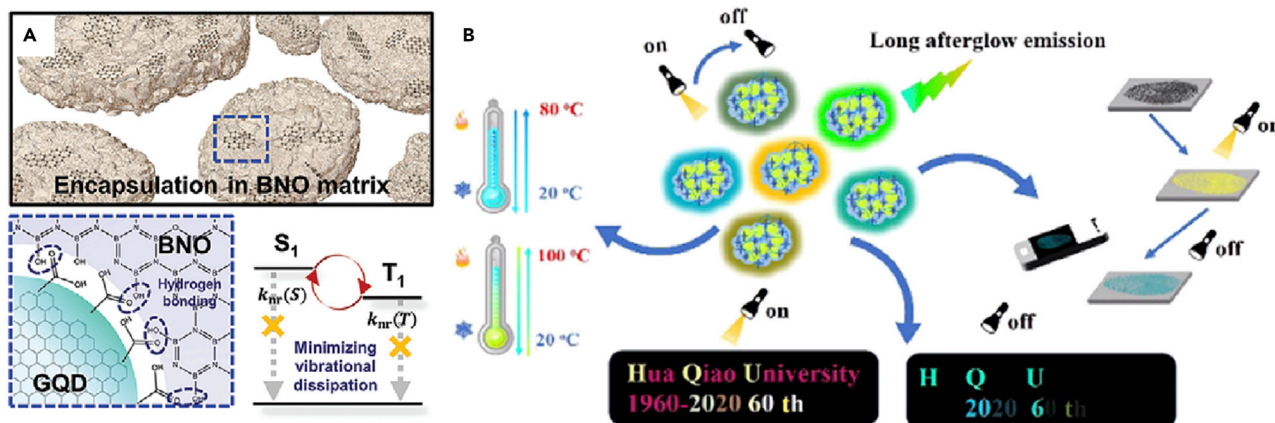


**Figure 8. BA-assisted CDs-based DF composites**

(A) Schematic illustration for the series of GQDs encapsulated in boron oxynitride (BNO) matrix to stabilize triplet excited states. Reproduced with the permission from (Park et al., 2020). Copyright 2020 Wiley-VCH.

(B) Schematic for the visible-light-excited multicolor afterglow of CDs in boron oxide applied to information encryption. Reproduced with the permission from (He et al., 2021). Copyright 2021 American Chemical Society.

Tan et al. (2016) introduced nitrogen-doped CQDs, which were synthesized using isophorone diisocyanate (IPDI) as single carbon source, into the PU matrix by the “monomer as solvent” strategy to synthesize the CQD/PU composite with RTP and DF at room temperature. PU matrix plays a critical role in inhibiting the triplet exciton non-radiative transition. As shown in Figure 9A, He, et al. (2018) synthesized CDs/PVA nanofibers by fixing CDs in PVA) via electrospinning. They exhibit good FL, RTP, and TADF properties. The mesoporous structure of the nanofibers can effectively stabilize the excited triplet state to inhibit oxygen quenching, which is conducive to the generation of TADF.

As a common organic matrix, urea will deaminate and condense during heating because of its thermal instability, and then form recrystallization urea, biuret, cyanuric acid or other organic compounds. Using urea as matrix, CDs can be embedded in composites formed by urea during the heating process to limit their non-radiative loss of the luminescence center. For example, Lin, et al. (2019) prepared the full-color and multi-emission CDs-based fluorescent ink with ultra-long afterglow by urea as the matrix through the “package-dissolution-recrystallization” strategy (Figure 9B). The nitrogen-doped CDs synthesized by hydrothermal method were first encapsulated by urea/biuret bonds to form NCD1-C composite, showing excitation-dependent afterglow. Under short-wavelength (254 nm) excitation, the composite exhibits DF whereas under long-wavelength (254 nm) excitation, it presents RTP. The DF property is consistent with the ISC between hot exciton systems. NCD1-C ink in DMF does not possess afterglow properties. After printing, the afterglow recovers. That is because DMF can be extracted by paper fiber can extract, promoting the rapid precipitation and recrystallization of urea. The hydrogen bonds formed between recrystallization urea/biuret and CDs inhibit the intermolecular vibration and diffusion movement. Moreover, the recrystallization framework can be used as a dense layer to isolate oxygen to reduce non-radiative relaxation, finally stabilizing the excited triplet state.

In addition to the above-mentioned inorganic and organic matrices, other reported matrices, such as nano-hydroxyapatite, metal nanoframes, metal-organic framework, and biopolymer cellulose derivatives, are also worth applying to the matrix-assisted systems (Zhao et al., 2015; Zhao et al., 2017; Miao et al., 2022; Riahi et al., 2022), which can further expand the types of CDs-based DF materials and endow them with diverse optical properties.

### Self-protective method

The self-protective CDs can be protected by the polymer-like structures, hydrogen bonds or supramolecular interactions on their surfaces, of which can form rigid protection to CDs, inhibiting the non-radiative transition to active afterglow emission. Self-protective method can largely improve the interface compatibility in matrix-assisted composites. Zou et al. (2016) obtained CDs with solid RTP by solvothermal reaction with 3-bromophenol as precursor. The RTP property originates from the formation of polymer-like CDs in

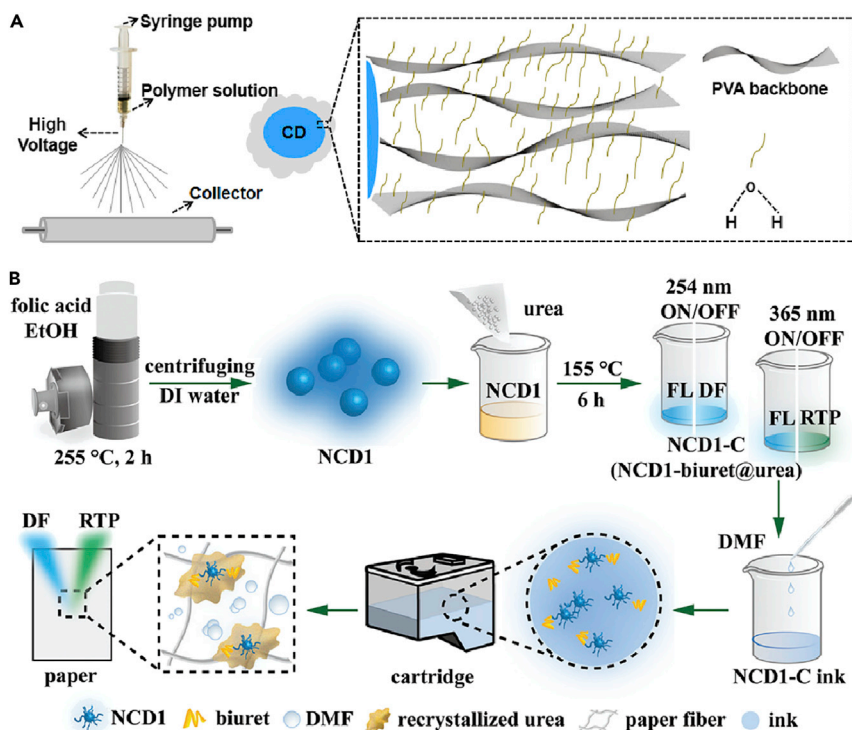


**Figure 9. Other matrix-assisted CDs-based DF composite materials**

(A) Schematic for the fabrication of nanofibers via electrospinning and the structure suggested for the nanofibers. Reproduced with the permission from (He et al., 2018). Copyright 2018 Elsevier.

(B) Schematic of the synthesis route of CD-based anti-counterfeiting ink. Reproduced with the permission from (Lin et al., 2019). Copyright 2019 Royal Society of Chemistry.

the reaction process. The polymer-like structures can stabilize the excited triplet state to avoid non-radiative relaxation. However, the triplet state is easily quenched by dissolved oxygen and water in the liquid phase. In order to effectively isolate oxygen and water in the atmosphere environment to stabilize the triplet state, Chen, et al. (2017) synthesized self-dispersed CPDs with cross-linking polymerization network by one-step using PVA as carbon source and EDA as nitrogen source. As shown in Figure 10A, the CPDs present aggregation-induced RTP property. Recently, Li, et al. (2019d) synthesized nitrogen-doped CDs (NCDs) by cross-linking polymerization, oxidation and dehydration with acrylamide, urea and citric acid as precursors (Figure 10B). Hydrogen bonds are formed by the reaction of polyacrylamide from acrylamide with citric acid and urea. The hydrogen bond protection can inhibit the triplet state from quenching in non-radiative way, finally the CDs emit long lifetime afterglow. Later, Xia, et al. (2020) used acrylamide as the precursor to obtain AN-CPDs after polymerization and carbonization under solvothermal conditions. In the aggregation state, the non-radiative transition of AN-CPDs is limited under the effect of supramolecular crosslinking, and thus the triplet state is stabilized.

Recently, Sun, et al. (2022) prepared a series of matrix-free CDs with the regulable afterglow between RTP and DF using six kinds of benzoic acid derivatives as precursors and ethylenediamine as crosslinking agent (Figure 10C). The afterglow emission of these self-protective CDs is activated by the polymer-like structure and N=C=O bonds, which are formed by the dehydration reaction between carboxyl group of benzoic acid derivatives and the amino group of ethylenediamine. The polymer-like structures can protect the triplet excitons. Obviously, the self-protected method can provide a simple preparation for CDs-based DF materials with stable afterglow.

### Energy difference regulation

The realization of DF depends on the energy level state of the excited triplet state. The energy difference regulation between the excited singlet and the triplet state has been studied in RTP system, such



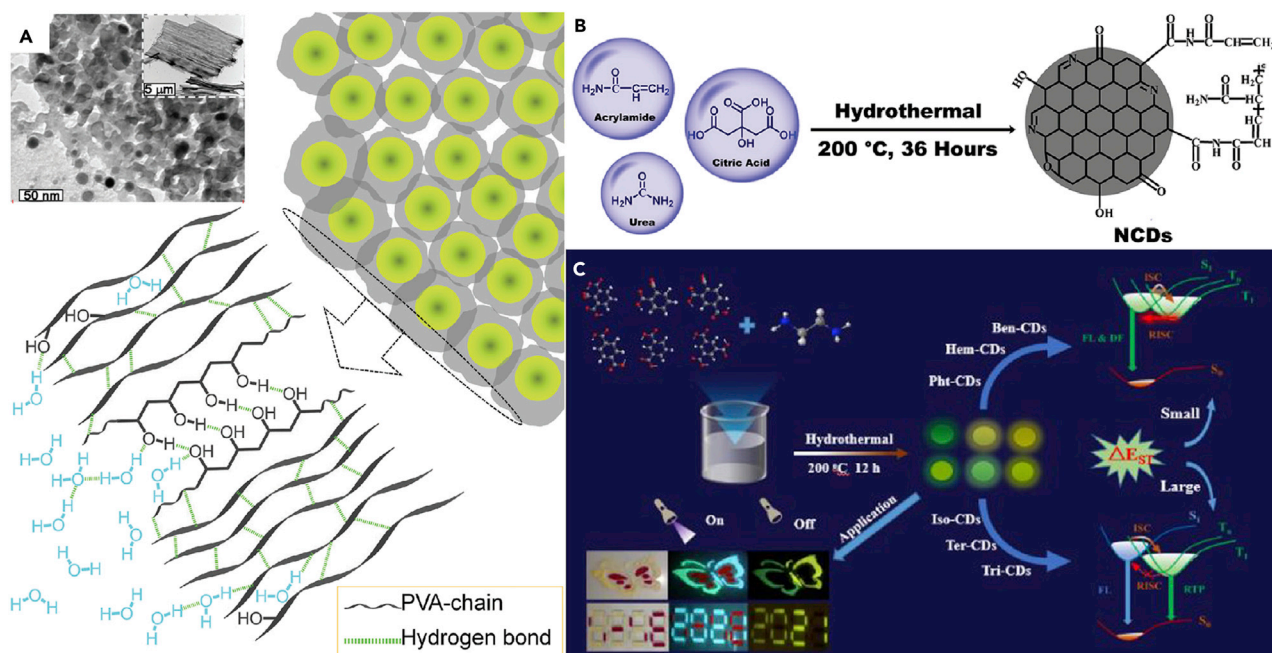


**Figure 10. Self-protective CDs-based afterglow materials**

(A) TEM image and schematic diagram of PVA-chain induced self-protective RTP emission. Reproduced with the permission from (Chen et al., 2017). Copyright 2017 Royal Society of Chemistry.

(B) A schematic of the procedure used for the preparation of NCDs. Reproduced with the permission from (Li et al., 2019d). Copyright 2019 Royal Society of Chemistry.

(C) Schematic diagram of self-protective CDs with tunable RTP and DF from six benzoic acid derivatives. Reproduced with the permission from (Sun et al., 2022). Copyright 2022 American Chemical Society.

as introducing electron-withdrawing atoms, increasing the donor-acceptor interaction, adjusting the fine structure, changing the cation and anion of the main inorganic phase and intramolecular electron coupling (Li et al., 2019c; Yang et al., 2018; Green et al., 2019; Ke et al., 2015; Henry and Siebrand, 1971). These regulation methods can also be applied to CDs-based DF materials to achieve energy difference regulation of CDs through adjusting the intrinsic structure of CDs or intra- or intermolecular forces on the surface of CDs. In the design and preparation of CDs-based composites DF, their appropriate intrinsic structural design can enhance the spin-orbit coupling to promote ISC process, and effective intra- or intermolecular interactions can form new band gap of CDs, which are beneficial to decreased  $\Delta E_{ST}$ . This section will discuss the influence factors on the  $\Delta E_{ST}$  of CDs-based DF composites from two aspects of intrinsic structural design and intermolecular interaction.

### Intrinsic structural design of CDs

The structure of CDs depends largely on raw materials and synthesis conditions. By controlling the carbon source, dopants and prepared technology of CDs, their intrinsic structure, such as  $sp^2$  conjugated domain, heteroatom doping content, electronic configuration, can be regulated, and finally the energy level state can be adjusted.

The  $sp^2$  conjugated domain is very important for the photoluminescence properties of CDs. Conjugate-induced DF refers to that the expansion of the conjugated system can effectively reduce the energy level splitting between the charge transfer states, which contributes to the decreased exchange splitting for effective  $\Delta E_{ST}$ . It has been studied in the TADF of polymers (Wei et al., 2017). Zhai et al. (2021) prepared a series of conjugated afterglow emission composite films on the basis of the conjugate-induced DF, and proposed that the large-conjugated system in the aromatic  $sp^2$  domain of carbon core reduce the band gap and promote DF emission. Among them, the CD2-H/PVA and CD2-OH/PVA composite films showed strong pure blue DF. The FL of the composite film can be tuned by alkali solution treatment. The DF ascribes from the carbon core with large  $\pi$ -conjugate system, which indicates that the introduction of aromatic precursors with  $\pi$ -bond into the preparation process of CDs can help DF emission.

For self-protective CDs-based afterglow materials, they are confined to RTP because DF depends on the coefficient of small  $\Delta E_{ST}$  and stable excited triplet states. Therefore, in order to obtain DF materials, the  $\Delta E_{ST}$  of self-protection CD-based afterglow materials also need to be reduced except the protection of excited triplet states by hydrogen bonds and other supramolecular interactions. Sun et al. (2022) regulated the  $\Delta E_{ST}$  of self-protective CDs by changing the substitution position of carboxyl group on the benzene ring, realizing the regulation between RTP and DF. When the carboxyl groups on the benzene ring of precursor have ortho-position substituent, it is more conducive to form six-membered rings to expand the rigid conjugated structure, thus reducing  $\Delta E_{ST}$  to generate DF.

The  $\Delta E_{ST}$  of CD@zeolite composites can be modulated through regulating the structure and energy level state of CDs by changing the solvents and organic structure-directing agents (Wang et al., 2019). Liu et al. (2019) *in-situ* synthesized different afterglow composites at room temperature by changing organic templates under the same solvent conditions. The CDs@SBT-1 composites prepared using 4-(2-aminoethyl) morpholine as template shows RTP characteristics whereas the CDs@SBT-2 composites prepared using TTDDA as template shows TADF characteristics. The  $\Delta E_{ST}$  of CDs@SBT-1 and CDs@SBT-2 composites are 0.36 and 0.18 eV, respectively, in which their different  $\Delta E_{ST}$  value is because of the different  $\Delta E_{ST}$  of CDs confined in matrix. Compared with the CDs@SBT-1, more C–O and C=O groups on the CDs in the CDs@SBT-2 mother solution lead to a larger steric hindrance structure, which achieves the spatially separated HOMO and LUMO, finally reducing  $\Delta E_{ST}$  (Tao et al., 2014).

Heteroatom doping is a common method to regulate the fluorescence properties of CDs. Because atoms containing lone-pair electrons such as O and N are beneficial to  $n-\pi^*$  transition, they can enhance spin orbit coupling (SOC) to reduce the band gap and promote ISC (Park et al., 2020). Therefore, the introduction of functional groups for promoting  $n-\pi^*$  transition in the structure of CDs is also one of main means to reduce  $\Delta E_{ST}$ . Hou et al. (2015) synthesized water-soluble CDs by microwave-assisted method in non-miscible system. The CDs present excitation-independent fluorescence and TADF at low temperature. Their excitation-independent FL is attributed to the non-radiative transition caused by the inherent band gap between the carbon core state and the surface state. The oxygen-containing functional group (C=O) on the surface of CDs can reduce  $\Delta E_{ST}$  to promote RISC through effective SOC (Dong et al., 2013), which is conducive to TADF. However, due to the quenching effect of oxygen on the excited triplet state, no TADF is observed at room temperature. When the CDs solution is frozen at low temperature, the C=O bonds on CDs become rigid, reducing the direct contact with oxygen, which activates the effective TADF. In view of heavy atoms doping such as Br, Cl, F can play a positive role to enhance the SOC, Mo, et al. (2021) reported the  $\Delta E_{ST}$  of F, NCDs@SiO<sub>2</sub> composites was reduced by fluorine doping to promote ISC and RISC, which are instrumental in generating TADF.

Previous studies have shown that the electron delocalization of GQDs effectively reduces the energy gap between the excited triplet and singlet states (Henry and Siebrand, 1971; Mueller et al., 2010; Bixon and Jortner, 1968; Lower and El-Sayed, 1966). For example, the vibration coupling of out-of-plane bending modes (C–H or C=C) can promote ISC, which is consistent with the effect of conjugated polycyclic aromatic hydrocarbons. However, these methods do not consider the oxidation effect, and is only suitable for GQDs prepared by bottom-up method, and their phosphorescence lifetime is short. A novel energy-level regulation strategy for up-bottom GQDs by introducing distorted structures to change the electronic configuration can not only improve the phosphorescence lifetime, but also realize TADF. Park et al. (2020) prepared a series of composite materials with adjustable RTP and TADF by changing the oxidation degree of oxygen-containing functional groups in GQD to regulate the  $\Delta E_{ST}$ . The increasing oxidation degree of oxygen functional groups induces the distorted structure, resulting in enhanced SOC and reduced  $\Delta E_{ST}$ , thus promoting the RISC and TADF.

#### *Construction of intra/intermolecular interactions*

During the combination of CDs and matrix, the abundant functional groups on the surface of CDs can form different intra/intermolecular interactions, such as,  $\pi-\pi$  interaction, energy transfer process, covalent bonds. Different types of intra/intermolecular interactions can not only limit CDs in rigid network structures, but also regulate their energy level states.

The introduction of electron-withdrawing groups can enhance  $\pi-\pi$  interaction, which can split the energy levels of LUMO and HOMO to produce a new excited state with lower energy, so as to reduce the energy

difference (Yang et al., 2018). Boron atoms, as the left neighbor of carbon atoms, attract  $\pi$ -electrons by their empty p-orbital to form p- $\pi$  conjugate system, which can effectively reduce the LUMO of the system (Wakamiya et al., 2006). The CDs-based composites using BA as the matrix use this strategy to reduce  $\Delta E_{ST}$ , and then a series of CDs/B<sub>2</sub>O<sub>3</sub> composites are prepared, showing TADF properties (Xu et al., 2020a; He et al., 2021).

In organic optoelectronics, the introduction of strong donors and acceptors is usually used to reduce  $\Delta E_{ST}$  (Wang, 2020). The donor-acceptor interaction can form energy transfer process between CDs to regulate the energy level of CDs. Zhang et al. (2020a) synthesized the composite materials with tunable TADF characteristics by the energy transfer between different CDs in zeolite matrix. TTDDA and *m*-phenylenediamine were used as organic templates to synthesize CDs with different structure and energy level: CD<sub>1</sub> and CD<sub>2</sub>. CD<sub>1</sub> was used as donor and CD<sub>2</sub> was used as acceptor, the energy transfer among CDs can form a new narrow band gap to reduce the  $\Delta E_{ST}$  for DF. The nano-space of zeolite makes the distance between donor and acceptor close enough to realize energy transfer (Johnson-Buck et al., 2013; Lutsyk et al., 2016; Wei et al., 2018). By changing the addition of *m*-phenylenediamine to regulate polymerization degree, which can obtain different functional groups on CDs acceptor, realizing the tunable TADF.

By introducing inorganic electron traps between the S<sub>1</sub> and T<sub>1</sub> state can also form energy transfer process to realize a new narrow band gap. He et al. (2020) synthesized CDs-based composites (CDs-SiO<sub>2</sub>), which emit enhanced phosphorescence and DF in solid and liquid phases by one-pot sol-gel method. The electron traps in SiO<sub>2</sub> matrix can act as electron transporter to capture, storage and release the electrons between S<sub>1</sub> and T<sub>1</sub> state, lowering the electron transfer processes and generating a small energy gap between the S<sub>1</sub> and electron trap state for long-lived DF.

In addition, the construction of covalent bonds between CDs and matrix can not only make CDs closely connected with matrix, but also reduce  $\Delta E_{ST}$ . Compared with the  $\Delta E_{ST}$  (0.5 eV) of *m*-CDs-PVA composites prepared by (Jiang et al., 2016) relying on hydrogen bonding, the formation of N-Si and C-Si covalent bonds can effectively reduce the  $\Delta E_{ST}$  (0.3 eV) of *m*-CDs@nSiO<sub>2</sub> composites prepared by Jiang et al. (2017), thus showing DF. Recently, (Wang et al., 2021b) embedded *o*-CDs from *o*-phenylenediamine into cyanuric acid from urine to realize the visible and near infrared dual glow emission of CDs-based composites at room temperature. The  $\Delta E_{ST}$  of *o*-CDs before and after embedding decreases from 0.594 to 0.481 eV, which indicates that the formation of covalent bonds can reduce  $\Delta E_{ST}$  and is the key to the dual afterglow emission of the composites.

## APPLICATIONS

Based on the long lifetime of DF materials without prompt excitation, they can be applied to the fields of information security. Some CDs-based DF composites are accompanied by RTP properties, this multiple afterglow emission provides more possibilities in the applications of anti-counterfeiting and information encryption. Moreover, CDs-based TADF materials are also applied to temperature sensing because of their excellent temperature-dependent optical properties. CDs-based DF composites also show enormous application potential in fingerprint detection, biological imaging, and other fields. The key observation and properties of CDs-based DF materials were summarized in the Table 2. The excited-dependent, temperature-dependent or water-simulated afterglow color of CDs-based DF materials can create multi-level security for anti-counterfeiting and information encryption. And the longer lifetime at naked eyes can more easily identify authenticity and information content. In addition, the temperature-dependent afterglow and lifetime of CDs-based DF materials provide a new protocol for the design of novel temperature sensor. Finally, the longer lifetime at naked eyes of CDs-based DF materials can provide more time to observe the cell situation and realize rapid detection, which also benefits for biological imaging and fingerprint detection.

### Anti-counterfeiting icons

For the modern commodity economy, a wide variety of industries have been plagued by commodity forgery. Many anti-counterfeiting strategies have emerged to identify the authenticity of commodities. The application of anti-counterfeiting icons increases the cost of forgery, which reduces the forgery rate. Among them, an FL labeling anti-counterfeiting technology has developed because of its convenience. However, single-mode FL anti-counterfeiting icons has gradually exposed a few disadvantages in recent years, such as easy to be copied, susceptible to FL interference from the background, and immediate

**Table 2. Applications of CDs-based DF materials**

Application	Afterglow color	Lifetime (naked eyes)	Temperature dependence	Remarks	Ref.
Anti-counterfeiting	Blue	1 s	100–350 K TADF↑	CDs@AIPO-5	(Liu et al., 2017)
	Blue-green	13 s	77–350 K TADF↑ RTP↓	G-CD/B <sub>2</sub> O <sub>3</sub>	(Xu et al., 2020a)
	Blue (254 nm Ex.) Green (365 nm Ex.)	6 s	80–320 K TADF↑ RTP↓	CDs@AIPO-5	(Deng et al., 2019)
	Blue (254 nm Ex.) Green (365 nm Ex.)	NA	303–433 K DF↓ (254 nm Ex.) TADF↑ RTP↓ (365 nm Ex)	NCD1-C	(Lin et al., 2019)
	Information encryption	Green (365 nm Ex.)	NA	100–300 K RTP↓	CDs@SBT-1
Information encryption	Blue (365 nm Ex.)	NA	100–300 K TADF↑	CDs@SBT-2	
	Blue (0)	1 s	80–305 K TADF↑	CD1@MgPO-5	(Zhang et al., 2020a)
	Cyan (0.007)	2 s		CD1 CD2@MgPO-5-a	
	Mint green (0.014)	3 s		CD1 CD2@MgPO-5-b	
	Olive green (0.042)	4 s		CD1 CD2@MgPO-5-c	
	Blue (drying) Green (wetting)	NA	77–298 K DF↓	TPA-CDs/Si	(Han et al., 2021)
	Blue	NA	298.15–423.15 K TADF↑	m-CDs@nSiO <sub>2</sub>	(Jiang et al., 2017)
	Green	10 s (Solid), 8 s (Liquid)	250–350 K TADF↑	F, NCDs@SiO <sub>2</sub>	(Mo et al., 2021)
Temperature sensing	Blue	NA	77–163 K TADF↓ 163–193 K TADF↑ 193–373 K TADF↓	CD@SiO <sub>2</sub>	(Liu et al., 2020)
	Green (Low temperature), Blue (High temperature)	11 s (Solid), 5 s (Liquid)	77–450 K TADF↑ RTP↓	CDs@SiO <sub>2</sub>	(Sun et al., 2020a)
	Green (Low temperature), Blue (High temperature)	20 s	80–400 K TADF↑	CDs-SiO <sub>2</sub>	(He et al., 2020)
Biological imaging	Green	10 s (Solid), 8 s (Liquid)	250–350 K TADF↑	F, NCDs@SiO <sub>2</sub>	(Mo et al., 2021)
Fingerprint detection	Blue-green	8 s	20–80°C TADF↑ RTP↓	CDs-l/B <sub>2</sub> O <sub>3</sub>	(He et al., 2021)
Light-emitting diodes	Green	10 s	80–320 K TADF↑	CDs@AIPO-5	(Zhang et al., 2020b)

NA: Not available; TADF: Thermally activated delayed fluorescence; RTP: Room temperature phosphorescence; DF: Delayed fluorescence.

excitation to be provided. The multi-mode anti-counterfeiting icons based on FL and afterglow (RTP and DF) is hard to copy because the FL and afterglow with different optical properties are combined, and the afterglow mode does not require immediate excitation to solve the problem of FL interference from the background. The long lifetime of afterglow mode can improve the anti-counterfeiting level. Therefore, the multi-mode anti-counterfeiting icon based on FL and afterglow has attracted extensive attention. The multiple afterglow emission properties of CDs-based DF composites make them stand out in the multi-mode anti-counterfeiting materials (Jiang et al., 2020b).

The CD@zeolite composites have opened up a broad new prospect for the application of DF. The continuous luminescence characteristics of TADF after stopping excitation can be used as another protection mode besides the traditional FL, namely the lifetime coding mode (Liu et al., 2017; Xu et al., 2020a). As shown in Figure 11A, (Liu et al., 2017) used CDs@2D-AIPO to draw the petal part of rose security icon, and phenol dye to draw the stem and leaf part. When excited by UV, the two parts emit blue and green FL, respectively. After removing the excitation source, the petal icon is still clearly visible. In addition, G-CD/B<sub>2</sub>O<sub>3</sub> composites prepared by Xu et al. (2020a) display blue-green fluorescence under 254 and 365 nm excitation, and yellow fluorescence under visible light. G-CD/starch composite shows yellow-green fluorescence under 254 nm excitation, blue-green FL under 365 nm excitation, and yellow FL under visible light. As shown in Figure 11B, the Yin fish and hexagrams drawn by G-CD/starch and G-CD/B<sub>2</sub>O<sub>3</sub> composites present different color patterns under 254 nm, 365 nm and visible light, respectively, indicating that this image security strategy can be applied to the practical anti-counterfeiting icon.

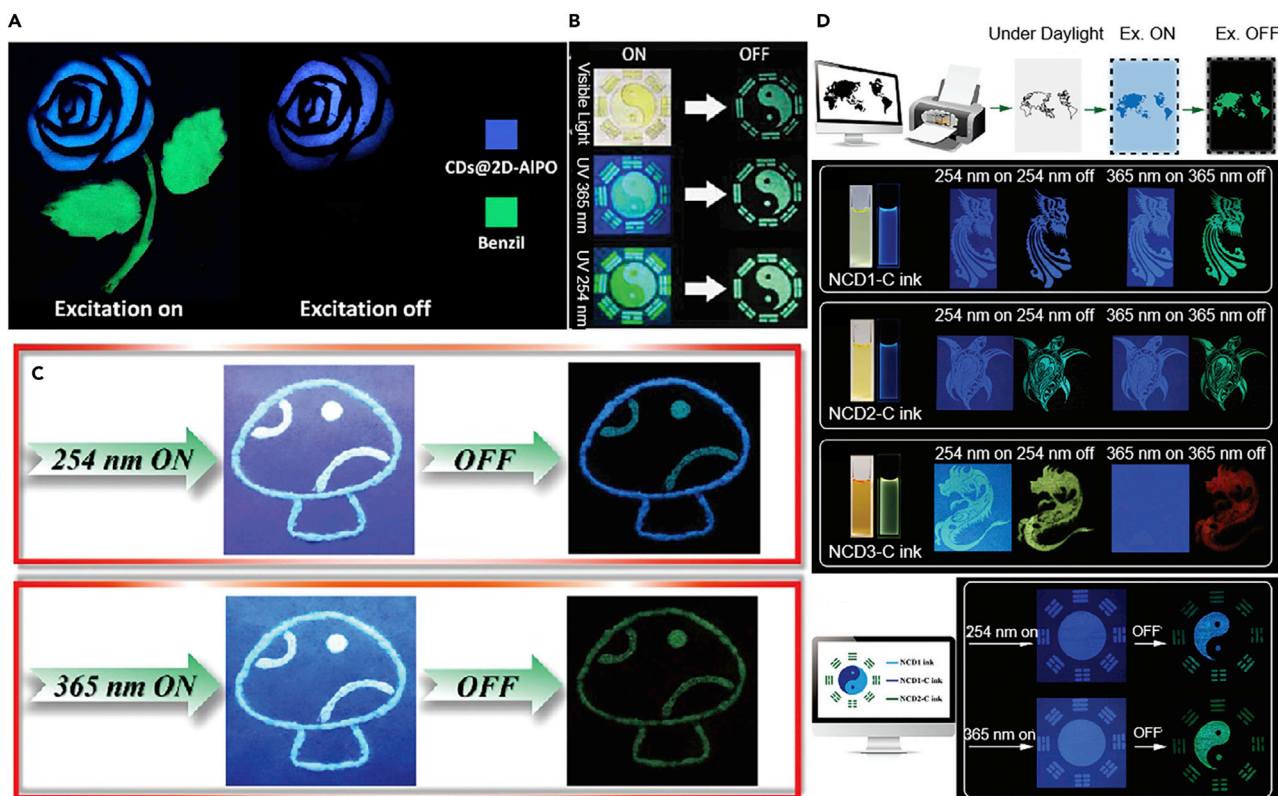


**Figure 11. CDs-based DF composites for anti-counterfeiting icons**

(A) Rose security icon: The security pattern of a rose is coded with the CDs@2D-AlPO as the flower part and the benzil dye molecule as the leaf and stem parts. Reproduced with the permission from (Liu et al., 2017). Copyright 2017 Science AAAS.

(B) Digital photos of graphic security made from the G-CD/B<sub>2</sub>O<sub>3</sub> composite and the G-CD/starch composite. Reproduced with the permission from (Xu et al., 2020a). Copyright 2020 Royal Society of Chemistry.

(C) Digital photographs of graphic security under excitation at 254 and 365 nm. Reproduced with the permission from (Deng et al., 2019). Copyright 2019 Royal Society of Chemistry.

(D) Schematic for optical anti-counterfeiting by inkjet printing and anti-counterfeiting ink application of multicolor afterglow of CD/heating urea system. Reproduced with the permission from (Lin et al., 2019). Copyright 2019 Royal Society of Chemistry.

The color tunable afterglow materials with triple emission (FL, RTP, and TADF) open up a novel way for advanced optical anti-counterfeiting applications. The mixed solution of CD@clay and PVA prepared by Deng et al. (2019) can be used as anti-counterfeiting ink to draw security icons. Because of excitation-dependent afterglow, the icons show different afterglow colors under irradiation off at different wavelengths, as shown in Figure 11C, which indicates that this kind of composites play a role in advanced anti-counterfeiting and data security. Lin et al. (2019) dissolve NCD1-C, NCD2-C, and NCD3-C in DMF to prepare the anti-counterfeiting ink, which is compatible with commercial inkjet printers (Figure 11D). When it is printed on paper, paper fibers can promote recrystallize rapidly, so that its afterglow performance is restored. The FL mode of the image acts under excitation source on. Once short-wavelength excitation is switched off, DF anti-counterfeiting mode starts to work whereas RTP anti-counterfeiting mode is opened after long-wavelength excitation stops. This triple-mode anti-counterfeiting strategy increases the difficulty of forgery, which is expected to be commercialized.

### Information encryption

With the rapid development of information society, the demand for information security is becoming more and more intense. Information encryption is a process of re-displaying hidden information under specific external stimulation. The photoluminescence behavior of materials can just meet this process. The traditional information encryption technology is based on the FL property. The FL lifetime is often short and easy to be interfered by the self-FL background, limiting its application. DF materials, which can continuously emit light, create a new way for information encryption technology. The photoluminescence diversity



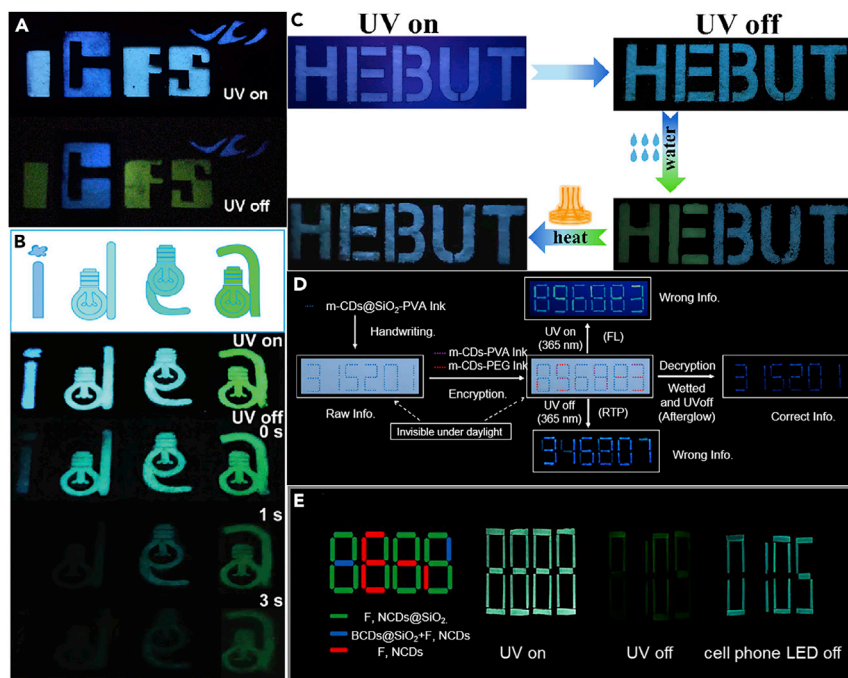


**Figure 12. CDs-based DF composites for information encryption**

- (A) Application of CDs@SBT-1 and CDs@SBT-2 in security protection. Reproduced with the permission from (Liu et al., 2019). Copyright 2019 American Chemical Society.
- (B) Multicolor display and time-dependent security protection of CD-based composites. Reproduced with the permission from (Zhang et al., 2020a). Copyright 2019 Royal Society of Chemistry.
- (C) Illustration of information encryption and decryption processes using TPA-CDs/Si via adding water and heating. Reproduced with the permission from (Han et al., 2021).
- (D) Schematic illustration of information protection processes by using *m*-CDs@nSiO<sub>2</sub>-PVA, *m*-CDs-PVA, and *m*-CDs-PEG inks. Reproduced with the permission from (Jiang et al., 2017).
- (E) Information encryption application based on F, NCDs@SiO<sub>2</sub> under UV. Reproduced with the permission from (Mo et al., 2021). Copyright 2021 Elsevier.

and environmental friendliness of CDs-based composites make them a kind of ideal materials for information encryption technology. Because the DF properties of CDs-based composites are mostly affected by excited triplet state that is sensitive to humidity and oxygen content, DF can realize multi-mode encryption, which further improve the information security and reliability compared with the ordinary fluorescent single-mode encryption.

CD@zeolite composites can be applied to the intelligent security protection by their triple coding modes with fluorescence, afterglow lifetime and afterglow color. For example, CDs@SBT-1, and CDs@SBT-2 are used to encrypt different information by Liu et al. (2019), as shown in Figure 12A. Blue FL security protection mode works under UV light. When UV excitation is off, the encryption part of CDs@SBT-1 shows green RTP mode whereas the encryption part of CDs@SBT-2 shows blue TADF mode. Based on the different color and lifetime of CD@zeolite composites caused by different CDs structures, Zhang, et al. (2020a) used CD<sub>1</sub>@MgAPO-5, CD<sub>1</sub>CD<sub>2</sub>@MgAPO-5-a, CD<sub>1</sub>CD<sub>2</sub>@MgAPO-5-b, and CD<sub>1</sub>CD<sub>2</sub>@MgAPO-5-c composites to realize multicolor display and time-dependent security protection. The security protection mode can be divided into "UV-on", "UV-off (instantly)", and "UV-off (for 1 and 3 s)". As shown in Figure 12B, the four letters "i", "d", "e", and "a" are fabricated by these four composites, respectively. Under UV light, the four composites display blue, green, menthol green, and olive green, respectively. After removing excitation for 1 s, "i", and "d" disappear, and only "e" is visible when it is extended to 3 s.

Based on the sensitivity of excited triplet states to water, Jiang, et al. (2017) used *m*-CDs@nSiO<sub>2</sub>-PVA, *m*-CDs-PVA, and *m*-CDs-PEG composites as DF, RTP, and ordinary FL inks to achieve a water-related information protection. As shown in Figure 12C, *m*-CDs@nSiO<sub>2</sub>-PVA are used for correct information, *m*-

CDs-PVA and *m*-CDs-PEG are used for error information. The error information written by RTP and FL inks are obtained with UV light on. After excitation stops, the error information under RTP mode is displayed, and only the correct information can be obtained under afterglow mode (DF) in moist environment. TPA-CD/Si prepared by Han et al. (2021) shows the water stimulus-responsive characteristics, which makes it possible to apply to advanced secure encryption. As shown in Figure 12D, "HEBUT" is encrypted by TPA-CD/Si powder, which emits blue fluorescence under a 254-nm UV lamp. After UV lamp is turned off, the blue DF of "HEBUT" last for several seconds, which is the first-order information encryption stage. After spraying some water on "HE", green afterglow opens when UV lamp is turned off, which is the secondary encryption process. The recovery of afterglow can be regarded as the decryption process, which is realized by heating the pattern with a 600°C heat gun for a short time.

Mo et al. (2021) realized advanced information encryption by combining the optical property of F, NCDs@SiO<sub>2</sub>, BCDs@SiO<sub>2</sub>, and F, NCDs. The F, NCDs@SiO<sub>2</sub> with visible-light-excited TADF can be used to decrypt the correct information. The BCDs@SiO<sub>2</sub> and F, NCDs are used as interference in encryption process. That is because the phosphorescence of BCDs@SiO<sub>2</sub> cannot be excited by visible light, and F, NCDs do not have afterglow property. As shown in Figure 12E the correct information (0105) is written by F, NCDs@SiO<sub>2</sub>. Under the irradiation of UV lamp, the error information (8888) is displayed, and another group of error information (8109) is displayed when the UV lamp is closed. Only when it is excited by visible light (mobile phone indicator) is the correct information displayed as (0105).

### Temperature sensing

Sensing is a technology that converts certain changes in the external environment or special substances into digital signals, so as to obtain information changes that people cannot perceive. Sensors are the core of sensing technology. Because of the universality of temperature measurement, the demand for the development of advanced temperature sensors is growing (Haro-Gonzalez et al., 2012). DF can effectively avoid the self-FL and scattering light of the substrate. Compared with the traditional FL method, the sensitivity of DF is higher. In addition, the intensity and lifetime of TADF are related to temperature, which means that DF materials have potential application prospects in the field of temperature sensing. Because most CDs-based DF composites are accompanied by phosphorescent emission properties, they provide a new choice for temperature sensing materials (Jiang et al., 2017).

The photoluminescence intensity of CD@SiO<sub>2</sub> composites prepared by Liu et al. (2020) shows a temperature-dependent in the range of 77–373 K, as shown in Figure 13A. The luminescent intensity decreases with the increase of temperature at 77–163 K and 193–373 K. At 163–193 K, DF is enhanced because of thermal activation, and the luminescent intensity increases with temperature. At 77–163 K and 193–373 K, the luminescent intensity of CD@SiO<sub>2</sub> composites has a good linear relationship with temperature. Therefore, CD@SiO<sub>2</sub> composite can be applied to photoluminescence intensity-based temperature sensing. Moreover, the composites have temperature-dependent lifetime based on long-lived TADF, which can be used as a high sensitivity nanothermometer for lifetime thermal sensing. When the temperature rises from 243 to 353 K, the lifetime of TADF decreases gradually. The lifetime and temperature can be described by equations. This thermal lifetime sensing does not need to consider the influence of excitation intensity or sensing material concentration. The nano-temperature sensing materials can extend the TADF lifetime to millisecond scale, which inhibits the interference from traditional short-lifetime FL background.

Because of the coexistence of RTP and TADF, the CDs@SiO<sub>2</sub> composites prepared by Sun et al. (2020a) are more sensitive to the change of temperature, and their temperature-dependent afterglow characteristics make them possible to become an alternative of temperature sensing materials. As shown in Figure 13B, in the temperature range of 233–333 K, the intensity ratio of phosphorescence (A<sub>1</sub>) to TADF (A<sub>2</sub>) is linearly correlated with temperature, and the luminescence thermometer based on this composite maintains a linear correlation with seasonal room temperature. Therefore, the CDs@SiO<sub>2</sub> composites are expected to be applied to the ratio-based temperature sensing field, which effectively eliminates the adverse effects such as self-FL interference and some human errors, improving the accuracy and sensitivity of sensors.

In addition, He, et al. (2020) first proposed a temperature sensor based on the color change of powdery CD-SiO<sub>2</sub>. The CD-SiO<sub>2</sub> composite gradually transforms from phosphorescence (green) to TADF (blue) with the increase of temperature. The tunable afterglow color and long afterglow lifetime visible to naked-eyes

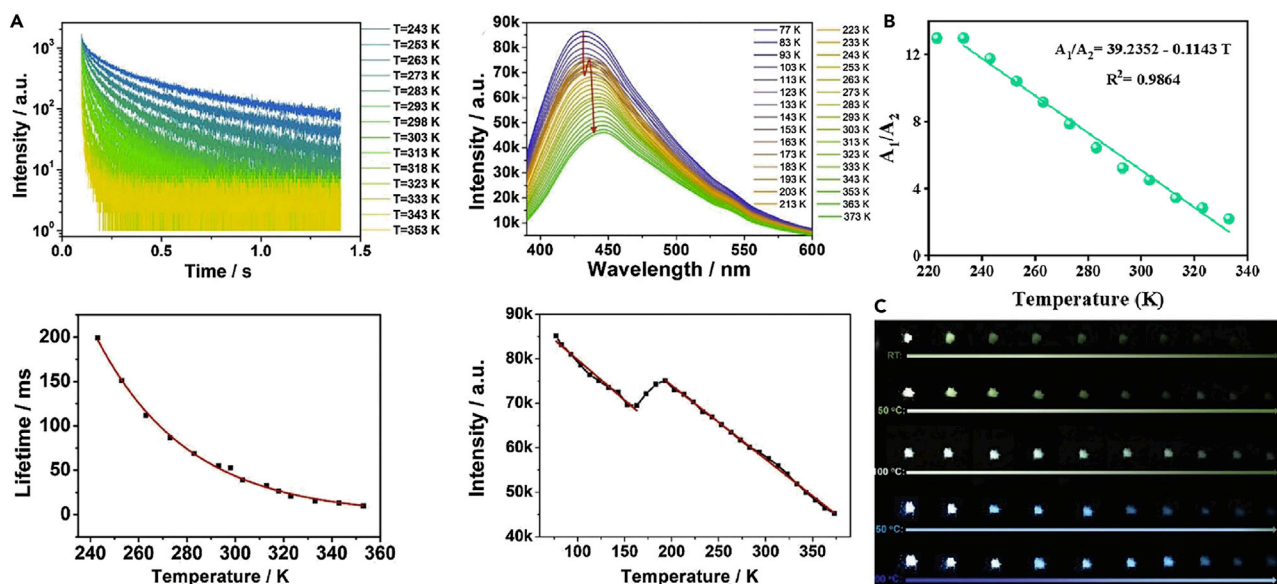


**Figure 13. CDs-based DF composites for temperature sensing**

(A) Temperature-responsive time-resolved decay spectra from 243 to 353 K and photoluminescence spectra from 77 to 373 K of CD@SiO<sub>2</sub>, and the fitting curves of temperature-dependent emission lifetime and emission intensity (the luminescent intensities centered at 440 nm) of CD@SiO<sub>2</sub>. Reproduced with the permission from (Liu et al., 2020). Copyright 2020 Elsevier.

(B) Temperature-dependent RTP/TADF emission ratio from 233 to 333 K of CDs@SiO<sub>2</sub>. Reproduced with the permission from (Sun et al., 2020a). Copyright 2020 Royal Society of Chemistry.

(C) The time-delayed afterglow color of powdery CDs-SiO<sub>2</sub> under various ambient temperatures. Reproduced with the permission from (He et al., 2020). Copyright 2020 Wiley-VCH.

(about 20 s) can provide a new possibility for realizing temperature sensing visualization. As shown in Figure 13C, by controlling heating temperature, the corresponding afterglow color changes from green to blue at room temperature, 50, 100, 150, and 200°C. The afterglow lifetime is long enough that naked eye can easily perceive the change of afterglow color, which make this temperature sensor reflect the temperature change more intuitively and quickly by color discrimination.

### Other applications

In addition to being used in anti-counterfeiting, information encryption, and temperature sensing, CDs-based DF composites have good development prospects in biological imaging, fingerprint detection, and light-emitting diodes.

Mo et al. (2021) presented that bright green FL signals were observed in human hepatocellular carcinoma cells (HepG2) incubated with F, NCDs@SiO<sub>2</sub> composites or F, NCDs under white laser excitation, and the FL images of both have high background, as shown in Figure 14A. However, the afterglow images of HepG2 cells containing F, NCDs@SiO<sub>2</sub> composites show low background signals due to DF. In addition, the white-light-excited F, NCDs@SiO<sub>2</sub> composites have stronger tissue permeability than other UV-excited CDs-based afterglow probes, so they are expected to be used as time-resolved bioimaging probes with low background signal and high signal-to-noise ratio. He et al. (2020) also used the RTP dominated CDs-based DF materials (CDs-SiO<sub>2</sub>) in the cellular imaging (Figure 14B). The FL intensity of HeLa cells embedded with CDs-SiO<sub>2</sub> was almost not reduced significantly after irradiation for 20 min. In addition, the CDs-SiO<sub>2</sub> nanoparticles did not need prompt excitation, which provides more potential for practical applications compared with commercial dye.

The traditional fingerprint detection technology based on FL powders has been quite mature, but it is still limited by the interference of FL from the background. Therefore, long-lifetime DF powder gradually shows its advantages in fingerprint detection. He et al. (2021) reported that the visible-light-excited CDs/B<sub>2</sub>O<sub>3</sub> composites can not only overcome the shortcomings of traditional fingerprint detection, but also does no harm to the human body. As shown in Figure 14C, the fingerprints on different substrates can be

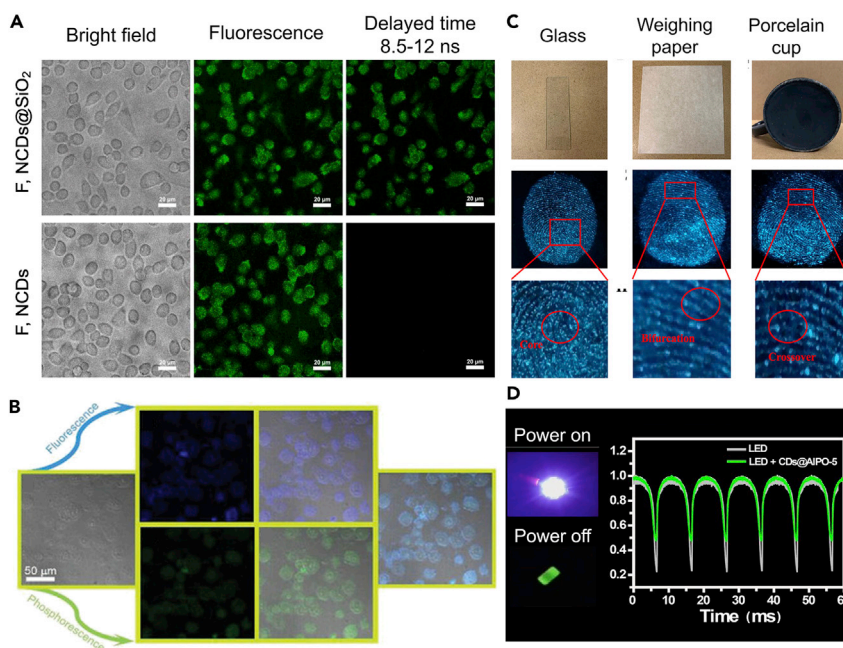


**Figure 14. CDs-based DF composites for bioimaging and fingerprint detection**

(A) The confocal images of HepG2 cells incubated with F, NCDs@SiO<sub>2</sub> and F, NCDs solutions, including bright field, fluorescence images and delayed fluorescence images (time-gated at 8.5–12 ns). Reproduced with the permission from (Mo et al., 2021). Copyright 2021 Elsevier.

(B) The confocal images of HeLa cells incubated with CDs-SiO<sub>2</sub> solution for 4 h. Reproduced with the permission from (He et al., 2020). Copyright 2020 Wiley-VCH.

(C) Visualization latent fingerprint detection with CDs-I/B<sub>2</sub>O<sub>3</sub> composites. Reproduced with the permission from (He et al., 2021). Copyright 2021 American Chemical Society.

(D) Luminescence intensity variations of the labeled light-emitting diodes devices driven in AC periodic cycles and photographs of light-emitting diodes device: power on, power off. Reproduced with the permission from (Zhang et al., 2020b). Copyright 2020 Chinese Chemical Society.

identified by CDs-I/B<sub>2</sub>O<sub>3</sub> composite powders after visible light excitation, and the fingerprint details are clear and identifiable. Remarkably, CDs-based DF materials have certain application potential in fingerprint visualization detection.

Zhang et al. (2020b) prepared an alternating-current light-emitting diode (AC LED) device with a cool white light by applying the CDs@AlPO-5 composites as phosphor powder (Figure 14D). The CIE coordinates of this device is (0.33, 0.34) with a correlated color temperature is 5462 K, and the color rendering index is 55. Notably, the calculated flicker percentage of this device is 70%, which is not harmful to human eyes and comparable with rare-earth metal-based phosphors. This work demonstrated the promising application of CDs-based DF materials in the AC LED supplementary lighting fields. Furthermore, CDs-based DF materials also have potential in the application of electroluminescence diodes. According to the generation process of DF, the red shift of emission peak position will not occur in DF process compared with RTP, which ensures high color purity. Moreover, the white emission diodes can be realized by using red, green, and blue DF materials as emitting layer, which will improve luminous efficiency compared with FL or FL/RTP diodes. Therefore, CDs-based DF materials are worth further developing and exploring their new applications.

## EXISTING CHALLENGES AND PROSPECTS

Although remarkable progress has been made in the research on the synthesis, structure and property adjusting, and diversified applications of CDs-based DF composites, there are still tremendous challenges for DF mechanism, synthesis and precise control strategies. As follows:

- (1) At present, the luminescence mechanism of CDs can be generally attributed to their carbon core states and surface states. However, there is lack of universal and clear explanation because the

fine structure of CDs cannot be determined. Therefore, the formation mechanism of CDs-based DF composites is not clear, which cannot effectively guide their directional synthesis and precise regulation.

- (2) Compared with RTP, CDs-based DF composites require smaller  $\Delta E_{ST}$ , therefore, their synthesis is relatively difficult. Small  $\Delta E_{ST}$  requires small spatial overlap between HOMO and LUMO, which decreases the radiation transition rate, resulting in low quantum yield (QY). Therefore, improving their QY as well as obtaining DF is one of the problems to be solved in the future.
- (3) The challenges of the preparation of CDs-based DF materials include the cumbersome purification process and low repetition rate, which limits large-scale commercial applications. For example, when amorphous  $\text{SiO}_2$  is used as the excited triplet stabilization matrix, the coating process of amorphous  $\text{SiO}_2$  on CDs is uncertain, which greatly reduces the product yield of CDs-based DF materials. Therefore, how to improve the product yield and repeatability is two of the future development directions of CDs-based DF materials. Although zeolite can be used as an effective and stable matrix to synthesize CDs-based DF materials, the strategy also has some limitations, such as longer preparation period of zeolite other matrices and limited carbon source precursors, which is also improved for zeolite as a stabilizing matrix.
- (4) Most of CDs-based DF composites present solid-state luminescence and emit blue DF, which greatly limits their application in multicolor displaying and bioimaging. Therefore, CDs-based DF materials with long-wavelength and liquid-phase DF are expected to be further developed.

Aiming at the above challenges, it is proposed that future attention for CDs-based DF materials be paid to the following aspects:

- (1) The specific photoluminescence mechanism of CDs needs to have a clear understanding of their structures, which requires us to systematically explore their common and different characteristics, and their structural evolution law in CDs synthesis process. Moreover, we also need to combine more advanced and comprehensive characterization methods (such as X-ray absorption near edge structure, mass spectrometry, transient absorption spectroscopy, and decay-dependent difference spectroscopy) with relevant simulating calculation methods (such as density functional theory calculation, time-dependent density functional theory calculation, hybrid quantum mechanics/molecular mechanics method, and independent gradient model) to explore and summarize the formation and PL mechanism of CDs-based composites, so as to further understand their DF source.
- (2) The coordination between small  $\Delta E_{ST}$  and high QY requires reasonable structural design. For example, the certain spatial steric hindrance between CDs can be introduced by matrix, while the geometric configurations are changed by regulating the functional groups. DF and higher QY can be simultaneously achieved by embedding CDs with aggregation-induced luminescence properties into the matrix.
- (3) In order to solve the existing problems in preparation process of CDs-based DF materials, a kind of new matrix with easy preparation and stable properties need to be developed. For example, the crystal encapsulation strategy will be explored for realizing the DF composite of CDs. The matrix-free self-protective CDs-based DF materials with intrinsic luminescence still need to be further improved to regulate the structure and the energy level state of CDs.
- (4) The CDs-based DF in liquid phase can be realized through embedding the CDs into the hydrophilic matrix. The long-wavelength of CDs can be achieved by surface modification, which can adjust the number and types of functional groups that are conducive to long-wavelength emission, thus promoting their application in biological imaging. The long lifetime of CDs-based DF materials is conducive to extending the diffusion distance of excitons before their dissociation and generating effective free charge, which are expected to be applied to the active layer for solar cells.

In summary, CDs-based DF composites possess the advantages of low cost, low toxicity, simple preparation process, stable luminescence, and so on. Therefore, they have incomparable superiority over other DF materials. In addition, their temperature dependence and multiple afterglow emission properties also make them a rising star in the application fields of temperature sensing, anti-counterfeiting encryption, fingerprint detection, biological imaging and other areas. Moreover, as a new type of DF materials,



CDs-based DF composites can effectively improve the inherent problems of traditional DF materials, and their long lifetime triplet state also gives them bright application prospect and development space in solar cells, photodynamic therapy, electroluminescent devices, and other fields. Nevertheless, there are still many problems that need to be further explored and solved in CDs-based DF materials, for example, the DF quenching of CDs-based DF materials prepared by matrix-assisted method when the matrix is destroyed by external environment (water, oxygen), the limited DF emission wavelength of CDs-based DF materials (mostly blue), and relative lower QY is induced by the smaller  $\Delta E_{ST}$ . Therefore, the novel CDs-based DF composites with environmental friendliness, economics, liquid stability and multicolor emission, and high QY should be explored in the future. The diverse applications of CDs-based DF materials can be achieved by combining CDs-based DF materials with other materials. For example, combining the chromic materials (such as photochromic, thermochromic, hydrochromic materials) with CDs-based DF materials will create multi-level authentication system of anti-counterfeiting and encryption, which can provide multiple simulations to confirm the authenticity, reduce forgery and enhance security. Perhaps, the smart polymer and other materials that respond to external stimuli such as air, water and temperature also can be accompanied with CDs-based DF composites to construct intelligent sensors with multi-dimensional response, high sensitivity and accuracy, which will reflect changes of the external environment more quickly and effectively. Moreover, the UV-absorption of CDs-based DF materials can be considered to apply to the UV-protection, the combination of CDs-based DF materials with UV-blocking films is expected to create a safer environment when UV light source is on. In the modern society with both opportunities and challenges, it is believed that CDs-based DF composites will become an advanced generation of luminescent materials in people's daily life through continuous attempts and efforts.

## ACKNOWLEDGMENTS

The authors in this work acknowledge the financial support from the National Natural Science Foundation of China (51972221, 61904121), Shanxi Scholarship Council of China (2020-051, HGKY2019027), Shanxi Zheda Institute of Advanced Materials and Chemical Engineering (2021SX-TD012) and Foundational Research Project of Shanxi Province (20210302123164, 20210302124604).

## AUTHOR CONTRIBUTIONS

Conceptualization, Y.Z.Y. and L.P.Y.; Investigation, M.X.L., Y.Z.Y., and L.P.Y.; Writing-Original Draft, M.X.L.; Writing Review & Editing, J.X.Z., Y.Z.Y., L.P.Y., X.G.L., and B.S.X.; Funding Acquisition, J.X.Z., L.P.Y., Y.Z.Y., and X.G.L.; Supervision, Y.Z.Y. and L.P.Y. All authors read and discussed the manuscript.

## DECLARATION OF INTERESTS

The authors declare no competing interests.

## REFERENCES

- Ali, H., Ghosh, S., and Jana, N.R. (2020). Fluorescent carbon dots as intracellular imaging probes. *Wiley Interdiscip. Rev. Nanomed. Nanobiotechnol.* 12, e1617. <https://doi.org/10.1002/wnan.1617>.
- An, Z., Zheng, C., Tao, Y., Chen, R., Shi, H., Chen, T., Wang, Z., Li, H., Deng, R., Liu, X., and Huang, W. (2015). Stabilizing triplet excited states for ultralong organic phosphorescence. *Nat. Mater.* 14, 685–690. <https://doi.org/10.1038/nmat4259>.
- Ashrafizadeh, M., Mohammadinejad, R., Kailasa, S.K., Ahmadi, Z., Afshar, E.G., and Pardakhty, A. (2020). Carbon dots as versatile nanoarchitectures for the treatment of neurological disorders and their theranostic applications: a review. *Adv. Colloid. Interface. Sci.* 278, 102123. <https://doi.org/10.1016/j.cis.2020.102123>.
- Atabaev, T.S. (2018). Doped carbon dots for sensing and bioimaging applications: a minireview. *Nanomaterials* 8, 342–352. <https://doi.org/10.3390/nano8050342>.
- Baldo, M.A., O'Brien, D.F., Thompson, M.E., and Forrest, S.R. (1999). Excitonic singlet-triplet ratio in a semiconducting organic thin film. *Phys. Rev. B* 60, 14422–14428. <https://doi.org/10.1103/PhysRevB.60.14422>.
- Bixon, M., and Jortner, J. (1968). Intramolecular radiationless transitions. *J. Chem. Phys.* 48, 715–726. <https://doi.org/10.1063/1.1668703>.
- Bos, A.J.J. (2017). Thermoluminescence as a research tool to investigate luminescence mechanisms. *Materials* 10, 1357–1379. <https://doi.org/10.3390/ma10121357>.
- Chen, Y., He, J., Hu, C., Zhang, H., Lei, B., and Liu, Y. (2017). Room temperature phosphorescence from moisture-resistant and oxygen-barred carbon dot aggregates. *J. Mater. Chem. C Mater.* 5, 6243–6250. <https://doi.org/10.1039/c7tc01615h>.
- Chiang, C.J., Kimyonok, A., Etherington, M.K., Griffiths, G.C., Jankus, V., Turksay, F., and Monkman, A.P. (2013). Ultrahigh efficiency fluorescent single and bi-layer organic light emitting diodes: the key role of triplet fusion. *Adv. Funct. Mater.* 23, 739–746. <https://doi.org/10.1002/adfm.201201750>.
- Deng, Y., Li, P., Jiang, H., Ji, X., and Li, H. (2019). Tunable afterglow luminescence and triple-mode emissions of thermally activated carbon dots confined within nanoclays. *J. Mater. Chem. C Mater.* 7, 13640–13646. <https://doi.org/10.1039/c9tc04863d>.
- Deng, Y., Zhao, D., Chen, X., Wang, F., Song, H., and Shen, D. (2013). Long lifetime pure organic phosphorescence based on water soluble carbon dots. *Chem. Commun.* 49, 5751–5753. <https://doi.org/10.1039/c3cc42600a>.
- Dias, F.B., Penfold, T.J., and Monkman, A.P. (2017). Photophysics of thermally activated delayed fluorescence molecules. *Methods Appl. Fluoresc.* 5, 012001. <https://doi.org/10.1088/2050-6120/aa537e>.
- Ding, Y., Zheng, J., Wang, J., Yang, Y., and Liu, X. (2019). Direct blending of multicolor carbon quantum dots into fluorescent films for white light

- emitting diodes with an adjustable correlated color temperature. *J. Mater. Chem. C Mater.* 7, 1502–1509. <https://doi.org/10.1039/c8tc04887h>.
- Dong, L., Xiong, Z., Liu, X., Sheng, D., Zhou, Y., and Yang, Y. (2019). Synthesis of carbon quantum dots to fabricate ultraviolet-shielding poly(vinylidene fluoride) films. *J. Appl. Polym. Sci.* 136, 47555. <https://doi.org/10.1002/app.47555>.
- Dong, X., Wei, L., Su, Y., Li, Z., Geng, H., Yang, C., and Zhang, Y. (2015). Efficient long lifetime room temperature phosphorescence of carbon dots in a potash alum matrix. *J. Mater. Chem. C Mater.* 3, 2798–2801. <https://doi.org/10.1039/c5tc00126a>.
- Dong, Y., Pang, H., Yang, H.B., Guo, C., Shao, J., Chi, Y., Li, C.M., and Yu, T. (2013). Carbon-based dots co-doped with nitrogen and sulfur for high quantum yield and excitation-independent emission. *Angew. Chem. Int. Ed. Engl.* 52, 7800–7804. <https://doi.org/10.1002/anie.201301114>.
- Feng, X., Zhao, Y., Jiang, Y., Miao, M., Cao, S., and Fang, J. (2017). Use of carbon dots to enhance UV-blocking of transparent nanocellulose films. *Carbohydr. Polym.* 161, 253–260. <https://doi.org/10.1016/j.carbpol.2017.01.030>.
- Gao, R., Kodaimati, M.S., and Yan, D. (2021). Recent advances in persistent luminescence based on molecular hybrid materials. *Chem. Soc. Rev.* 50, 5564–5589. <https://doi.org/10.1039/d0cs01463j>.
- Ghosh, S., Gul, A.R., Park, C.Y., Kim, M.W., Xu, P., Baek, S.H., Bhamore, J.R., Kailasa, S.K., and Park, T.J. (2021a). Facile synthesis of carbon dots from tagetes erecta as a precursor for determination of chlorpyrifos via fluorescence turn-off and quinalphos via fluorescence turn-on mechanisms. *Chemosphere* 279, 130515. <https://doi.org/10.1016/j.chemosphere.2021.130515>.
- Ghosh, S., Gul, A.R., Park, C.Y., Xu, P., Baek, S.H., Bhamore, J.R., Kim, M.W., Lee, M., Kailasa, S.K., and Park, T.J. (2021b). Green synthesis of carbon dots from calotropis procera leaves for trace level identification of isoprothiolane. *Microchem. J.* 167, 106272. <https://doi.org/10.1016/j.microc.2021.106272>.
- Godumala, M., Choi, S., Cho, M.J., and Choi, D.H. (2016). Thermally activated delayed fluorescence blue dopants and hosts: from the design strategy to organic light-emitting diode applications. *J. Mater. Chem. C Mater.* 4, 11355–11381. <https://doi.org/10.1039/c6tc04377a>.
- Green, D.C., Holden, M.A., Levenstein, M.A., Zhang, S., Johnson, B.R.G., Gala de Pablo, J., Ward, A., Botchway, S.W., and Meldrum, F.C. (2019). Controlling the fluorescence and room-temperature phosphorescence behaviour of carbon nanodots with inorganic crystalline nanocomposites. *Nat. Commun.* 10, 206–219. <https://doi.org/10.1038/s41467-018-08214-6>.
- Han, Z., Li, P., Deng, Y., and Li, H. (2021). Reversible and color-variable afterglow luminescence of carbon dots triggered by water for multi-level encryption and decryption. *Chem. Eng. J.* 415, 128999. <https://doi.org/10.1016/j.cej.2021.128999>.
- Haro-González, P., Martínez-Maestro, L., Martín, I.R., García-Solé, J., and Jaque, D. (2012). High-sensitivity fluorescence lifetime thermal sensing based on CdTe quantum dots. *Small* 8, 2652–2658. <https://doi.org/10.1002/sml.201102736>.
- He, J., Chen, Y., He, Y., Xu, X., Lei, B., Zhang, H., Zhuang, J., Hu, C., and Liu, Y. (2020). Anchoring carbon nanodots onto nanosilica for phosphorescence enhancement and delayed fluorescence nasecence in solid and liquid states. *Small* 16, e2005228. <https://doi.org/10.1002/sml.202005228>.
- He, J., He, Y., Chen, Y., Zhang, X., Hu, C., Zhuang, J., Lei, B., and Liu, Y. (2018). Construction and multifunctional applications of carbon dots/PVA nanofibers with phosphorescence and thermally activated delayed fluorescence. *Chem. Eng. J.* 347, 505–513. <https://doi.org/10.1016/j.cej.2018.04.110>.
- He, W., Sun, X., and Cao, X. (2021). Construction and multifunctional applications of visible-light-excited multicolor long afterglow carbon dots/boron oxide composites. *ACS Sustain. Chem. Eng.* 9, 4477–4486. <https://doi.org/10.1021/acssuschemeng.0c08652>.
- Henry, B.R., and Siebrand, W. (1971). Spin-orbit coupling in aromatic hydrocarbons. Analysis of nonradiative transitions between singlet and triplet states in benzene and naphthalene. *J. Chem. Phys.* 54, 1072–1085. <https://doi.org/10.1063/1.1674940>.
- Hou, J., Wang, L., Zhang, P., Xu, Y., and Ding, L. (2015). Facile synthesis of carbon dots in an immiscible system with excitation-independent emission and thermally activated delayed fluorescence. *Chem. Commun.* 51, 17768–17771. <https://doi.org/10.1039/c5cc08152a>.
- Hu, D., Yao, L., Yang, B., and Ma, Y. (2015). Reverse intersystem crossing from upper triplet levels to excited singlet: a 'hot excitation' path for organic light-emitting diodes. *Philos. Trans. A Math. Phys. Eng. Sci.* 373, 20140318. <https://doi.org/10.1098/rsta.2014.0318>.
- Jiang, K., Wang, Y., Cai, C., and Lin, H. (2017). Activating room temperature long afterglow of carbon dots via covalent fixation. *Chem. Mater.* 29, 4866–4873. <https://doi.org/10.1021/acs.chemmater.7b00831>.
- Jiang, K., Wang, Y., Li, Z., and Lin, H. (2020b). Afterglow of carbon dots: mechanism, strategy and applications. *Mater. Chem. Front.* 4, 386–399. <https://doi.org/10.1039/c9qm00578a>.
- Jiang, K., Zhang, L., Lu, J., Xu, C., Cai, C., and Lin, H. (2016). Triple-mode emission of carbon dots: applications for advanced anti-counterfeiting. *Angew. Chem. Int. Ed. Engl.* 55, 7231–7235. <https://doi.org/10.1002/anie.201602445>.
- Jiang, X., Tang, X., Tang, L., Zhang, B., and Mao, H. (2019). Synthesis and formation mechanism of amorphous silica particles via sol-gel process with tetraethylorthosilicate. *Ceram. Int.* 45, 7673–7680. <https://doi.org/10.1016/j.ceramint.2019.01.067>.
- Jiang, Y., Zhang, X., Xiao, L., Yan, R., Xin, J., Yin, C., Jia, Y., Zhao, Y., Xiao, C., Zhang, Z., and Song, W. (2020a). Preparation of dual-emission polyurethane/carbon dots thermoresponsive composite films for colorimetric temperature sensing. *Carbon* 163, 26–33. <https://doi.org/10.1016/j.carbon.2020.03.013>.
- Johnson-Buck, A.E., Blanco, M.R., and Walter, N.G. (2013). Single-molecule fluorescence resonance energy transfer. In *Encyclopedia of biophysics*, G.C.K. Roberts, ed. (Springer Berlin Heidelberg Roberts), pp. 2329–2335.
- Joseph, J., and Anappara, A.A. (2017). Cool white, persistent room-temperature phosphorescence in carbon dots embedded in a silica gel matrix. *Phys. Chem. Chem. Phys.* 19, 15137–15144. <https://doi.org/10.1039/c7cp02731a>.
- Ju, B., Nie, H., Liu, Z., Xu, H., Li, M., Wu, C., Wang, H., and Zhang, S.X.A. (2017). Full-colour carbon dots: integration of multiple emission centres into single particles. *Nanoscale* 9, 13326–13333. <https://doi.org/10.1039/c7nr04576j>.
- Kailasa, S.K., and Koduru, J.R. (2022). Perspectives of magnetic nature carbon dots in analytical chemistry: from separation to detection and bioimaging. *Trends Environ. Anal. Chem.* 33, e00153. <https://doi.org/10.1016/j.teac.2021.e00153>.
- Kang, H.X., Zheng, J.X., Liu, X.G., and Yang, Y.Z. (2021). Phosphorescent carbon dots: microstructure design, synthesis and applications. *N. Carbon Mater.* 36, 649–664. [https://doi.org/10.1016/s1872-5805\(21\)60083-5](https://doi.org/10.1016/s1872-5805(21)60083-5).
- Katsurada, Y., Hirata, S., Totani, K., Watanabe, T., and Vacha, M. (2015). Photoreversible on-off recording of persistent room-temperature phosphorescence. *Adv. Opt. Mater.* 3, 1726–1737. <https://doi.org/10.1002/adom.201500334>.
- Ke, X.S., Zhao, H., Zou, X., Ning, Y., Cheng, X., Su, H., and Zhang, J.L. (2015). Fine-tuning of beta-substitution to modulate the lowest triplet excited states: a bioinspired approach to design phosphorescent metalloporphyrinoids. *J. Am. Chem. Soc.* 137, 10745–10752. <https://doi.org/10.1021/jacs.5b06332>.
- Kousheh, S.A., Moradi, M., Tajik, H., and Molaei, R. (2020). Preparation of antimicrobial/ultraviolet protective bacterial nanocellulose film with carbon dots synthesized from lactic acid bacteria. *Int. J. Biol. Macromol.* 155, 216–225. <https://doi.org/10.1016/j.jbiomac.2020.03.230>.
- Li, H., Ye, S., Guo, J.Q., Kong, J.T., Song, J., Kang, Z.H., and Qu, J.L. (2019d). The design of room-temperature-phosphorescent carbon dots and their application as a security ink. *J. Mater. Chem. C Mater.* 7, 10605–10612. <https://doi.org/10.1039/c9tc03481a>.
- Li, J., Corma, A., and Yu, J. (2015). Synthesis of new zeolite structures. *Chem. Soc. Rev.* 44, 7112–7127. <https://doi.org/10.1039/c5cs00023h>.
- Li, J., Wang, B., Zhang, H., and Yu, J. (2019a). Carbon dots-in-matrix boosting intriguing luminescence properties and applications. *Small* 15, e1805504. <https://doi.org/10.1002/sml.201805504>.
- Li, W., Wu, S., Xu, X., Zhuang, J., Zhang, H., Zhang, X., Hu, C., Lei, B., Kaminski, C.F., and Liu, Y. (2019b). Carbon dot-silica nanoparticle composites for ultralong lifetime phosphorescence imaging in tissue and cells at room temperature. *Chem. Mater.* 31, 9887–9894. <https://doi.org/10.1021/acs.chemmater.9b04120>.

- Li, W., Zhou, W., Zhou, Z., Zhang, H., Zhang, X., Zhuang, J., Liu, Y., Lei, B., and Hu, C. (2019c). A universal strategy for activating the multicolor room-temperature afterglow of carbon dots in a boric acid matrix. *Angew. Chem. Int. Ed. Engl.* 58, 7278–7283. <https://doi.org/10.1002/anie.201814629>.
- Li, X., Cao, F., Yu, D., Chen, J., Sun, Z., Shen, Y., Zhu, Y., Wang, L., Wei, Y., Wu, Y., and Zeng, H. (2017). All inorganic halide perovskites nanosystem: synthesis, structural features, optical properties and optoelectronic applications. *Small* 13, 1603996. <https://doi.org/10.1002/asm.201603996>.
- Lin, C., Zhuang, Y., Li, W., Zhou, T.L., and Xie, R.J. (2019). Blue, green, and red full-color ultralong afterglow in nitrogen-doped carbon dots. *Nanoscale* 11, 6584–6590. <https://doi.org/10.1039/c8nr09672d>.
- Lin, L.P., Wang, X.X., Lin, S.Q., Zhang, L.H., Lin, C.Q., Li, Z.M., and Liu, J.M. (2012). Research on the spectral properties of luminescent carbon dots. *Spectrochim. Acta Mol. Biomol. Spectrosc.* 95, 555–561. <https://doi.org/10.1016/j.saa.2012.04.049>.
- Liu, J., Kang, X., Zhang, H., Liu, Y., Wang, C., Gao, X., and Li, Y. (2020). Carbon dot-based nanocomposite: long-lived thermally activated delayed fluorescence for lifetime thermal sensing. *Dyes Pigment.* 181, 108576. <https://doi.org/10.1016/j.dyepig.2020.108576>.
- Liu, J., Wang, N., Yu, Y., Yan, Y., Zhang, H., Li, J., and Yu, J. (2017). Carbon dots in zeolites: a new class of thermally activated delayed fluorescence materials with ultralong lifetimes. *Sci. Adv.* 3, e1603171. <https://doi.org/10.1126/sciadv.1603171>.
- Liu, J., Zhang, H., Wang, N., Yu, Y., Cui, Y., Li, J., and Yu, J. (2019). Template-modulated afterglow of carbon dots in zeolites: room-temperature phosphorescence and thermally activated delayed fluorescence. *ACS Mater. Lett.* 1, 58–63. <https://doi.org/10.1021/acsmaterialslett.9b00073>.
- Lower, S.K., and El-Sayed, M.A. (1966). The triplet state and molecular electronic processes in organic molecules. *Chem. Rev.* 66, 199–241. <https://doi.org/10.1021/cr60240a004>.
- Lutsyk, P., Arif, R., Hrubby, J., Bukivskiy, A., Vinichuk, O., Shandura, M., Yakubovskiy, V., Kovtun, Y., Rance, G.A., Fay, M., et al. (2016). A sensing mechanism for the detection of carbon nanotubes using selective photoluminescent probes based on ionic complexes with organic dyes. *Light Sci. Appl.* 5, e16028. <https://doi.org/10.1038/lsa.2016.28>.
- Matsuzawa, T., Aoki, Y., Takeuchi, N., and Murayama, Y. (1996). A new long phosphorescent phosphor with high brightness, SrAl<sub>2</sub>O<sub>4</sub>: Eu<sup>2+</sup>, Dy<sup>3+</sup>. *J. Electrochem. Soc.* 143, 2670–2673. <https://doi.org/10.1002/chin.199649270>.
- Miao, M., Mu, L., Cao, S., Yang, Y., and Feng, X. (2022). Dual-functional CDs@ZIF-8/chitosan luminescent film sensors for simultaneous detection and adsorption of tetracycline. *Carbohydr. Polym.* 291, 119587. <https://doi.org/10.1016/j.carbpol.2022.119587>.
- Mo, L., Xu, X., Liu, Z., Liu, H., Lei, B., Zhuang, J., Guo, Z., Liu, Y., and Hu, C. (2021). Visible-light excitable thermally activated delayed fluorescence in aqueous solution from F, N-doped carbon dots confined in silica nanoparticles. *Chem. Eng. J.* 426, 130728. <https://doi.org/10.1016/j.cej.2021.130728>.
- Mueller, M.L., Yan, X., McGuire, J.A., and Li, L.S. (2010). Triplet states and electronic relaxation in photoexcited graphene quantum dots. *Nano Lett.* 10, 2679–2682. <https://doi.org/10.1021/nl101474d>.
- Park, M., Kim, H.S., Yoon, H., Kim, J., Lee, S., Yoo, S., and Jeon, S. (2020). Controllable singlet-triplet energy splitting of graphene quantum dots through oxidation: from phosphorescence to TADF. *Adv. Mater.* 32, e2000936. <https://doi.org/10.1002/adma.202000936>.
- Qu, D., and Sun, Z. (2020). The formation mechanism and fluorophores of carbon dots synthesized via a bottom-up route. *Mater. Chem. Front.* 4, 400–420. <https://doi.org/10.1039/c9qm00552h>.
- Riahi, Z., Rhim, J.W., Bagheri, R., Pircheraghi, G., and Lotfali, E. (2022). Carboxymethyl cellulose-based functional film integrated with chitosan-based carbon quantum dots for active food packaging applications. *Prog. Org. Coat.* 166, 106794. <https://doi.org/10.1016/j.porgcoat.2022.106794>.
- Salla, C.A.M., Farias, G., Rouzières, M., Dechambenoit, P., Durola, F., Bock, H., de Souza, B., and Bechtold, I.H. (2019). Persistent solid-state phosphorescence and delayed fluorescence at room temperature by a twisted hydrocarbon. *Angew. Chem. Int. Ed. Engl.* 58, 6982–6986. <https://doi.org/10.1002/anie.201901672>.
- Sun, X., He, W., and Liu, B. (2022). Regulation between the delayed fluorescence and room-temperature phosphorescence of matrix-free carbon dots with the position of the carboxyl substituent on the benzene ring. *J. Phys. Chem. C* 126, 3540–3548. <https://doi.org/10.1021/acs.jpcc.1c10159>.
- Sun, Y., Liu, J., Pang, X., Zhang, X., Zhuang, J., Zhang, H., Hu, C., Zheng, M., Lei, B., and Liu, Y. (2020a). Temperature-responsive conversion of thermally activated delayed fluorescence and room-temperature phosphorescence of carbon dots in silica. *J. Mater. Chem. C Mater.* 8, 5744–5751. <https://doi.org/10.1039/d0tc00507j>.
- Sun, Y., Zhang, X., Zhuang, J., Zhang, H., Hu, C., Zheng, M., Lei, B., and Liu, Y. (2020b). The room temperature afterglow mechanism in carbon dots: current state and further guidance perspective. *Carbon* 165, 306–316. <https://doi.org/10.1016/j.carbon.2020.04.030>.
- Tan, J., Zou, R., Zhang, J., Li, W., Zhang, L., and Yue, D. (2016). Large-scale synthesis of n-doped carbon quantum dots and their phosphorescence properties in a polyurethane matrix. *Nanoscale* 8, 4742–4747. <https://doi.org/10.1039/c5nr08516k>.
- Tang, G., Zhang, K., Feng, T., Tao, S., Han, M., Li, R., Wang, C., Wang, Y., and Yang, B. (2019). One-step preparation of silica microspheres with super-stable ultralong room temperature phosphorescence. *J. Mater. Chem. C Mater.* 7, 8680–8687. <https://doi.org/10.1039/c9tc02353d>.
- Tao, Y., Yuan, K., Chen, T., Xu, P., Li, H., Chen, R., Zheng, C., Zhang, L., and Huang, W. (2014). Thermally activated delayed fluorescence materials towards the breakthrough of organoelectronics. *Adv. Mater.* 26, 7931–7958. <https://doi.org/10.1002/adma.201402532>.
- Tetsuka, H., Asahi, R., Nagoya, A., Okamoto, K., Tajima, I., Ohta, R., and Okamoto, A. (2012). Optically tunable amino-functionalized graphene quantum dots. *Adv. Mater.* 24, 5333–5338. <https://doi.org/10.1002/adma.201201930>.
- Wakamiya, A., Taniguchi, T., and Yamaguchi, S. (2006). Intramolecular B–N coordination as a scaffold for electron-transporting materials: synthesis and properties of boryl-substituted thienylthiazoles. *Angew. Chem.* 118, 3242–3245. <https://doi.org/10.1002/ange.200504391>.
- Wang, B., Mu, Y., Zhang, H., Shi, H., Chen, G., Yu, Y., Yang, Z., Li, J., and Yu, J. (2019). Red room-temperature phosphorescence of CDs@zeolite composites triggered by heteroatoms in zeolite frameworks. *ACS Cent. Sci.* 5, 349–356. <https://doi.org/10.1021/acscentsci.8b00844>.
- Wang, J.L., Wang, Y.L., Zheng, J.X., Yu, S.P., Yang, Y.Z., and Liu, X.G. (2018b). Mechanism, tuning and application of excitation-dependent fluorescence property in carbon dots. *Prog. Chem.* 30, 1186–1201. <https://doi.org/10.7539/pc180103>.
- Wang, J., Zhang, F., Wang, Y., Yang, Y., and Liu, X. (2018a). Efficient resistance against solid-state quenching of carbon dots towards white light emitting diodes by physical embedding into silica. *Carbon* 126, 426–436. <https://doi.org/10.1016/j.carbon.2017.10.041>.
- Wang, X., Sun, X., Guan, X., Wang, Y., Chen, X., and Liu, X. (2021a). Tannic interfacial linkage within ZnO-loaded fabrics for durable UV-blocking applications. *Appl. Surf. Sci.* 568, 150960. <https://doi.org/10.1016/j.apsusc.2021.150960>.
- Wang, Y., Jiang, K., Du, J., Zheng, L., Li, Y., Li, Z., and Lin, H. (2021b). Green and near-infrared dual-mode afterglow of carbon dots and their applications for confidential information readout. *Nano-Micro Lett.* 13, 198. <https://doi.org/10.1007/s40820-021-00718-z>.
- Wang, Y.S. (2020). Study and analysis of thermal activation delay fluorescent materials. *Chem. Eng. Des. Commun.* 46, 130–131. <https://doi.org/10.3969/j.issn.1003-6490.2020.01.090>.
- Wang, Z., Yu, J., and Xu, R. (2012). Needs and trends in rational synthesis of zeolitic materials. *Chem. Soc. Rev.* 41, 1729–1741. <https://doi.org/10.1039/c1cs15150a>.
- Wei, Q., Fei, N., Islam, A., Lei, T., Hong, L., Peng, R., Fan, X., Chen, L., Gao, P., and Ge, Z. (2018). Small-molecule emitters with high quantum efficiency: mechanisms, structures, and applications in OLED devices. *Adv. Opt. Mater.* 6, 1800512. <https://doi.org/10.1002/adom.201800512>.
- Wei, Q., Kleine, P., Karpov, Y., Qiu, X., Komber, H., Sahre, K., Kiriya, A., Lygaitis, R., Lenk, S., Reineke, S., and Voit, B. (2017). Conjugation-induced thermally activated delayed fluorescence (TADF): from conventional non-tadf units to tadf-active polymers. *Adv. Funct. Mater.*

27, 1605051. <https://doi.org/10.1002/adfm.201605051>.

Xia, C., Zhu, S., Zhang, S.T., Zeng, Q., Tao, S., Tian, X., Li, Y., and Yang, B. (2020). Carbonized polymer dots with tunable room-temperature phosphorescence lifetime and wavelength. *ACS Appl. Mater. Interfaces* 12, 38593–38601. <https://doi.org/10.1021/acsami.0c11867>.

Xiao, L.X., and Zhang, C.F. (2020). Triplet excited states in organic luminescent materials. *Prog. Phys.* 40, 44–53. <https://doi.org/10.13725/j.cnki.pip.2020.02.002>.

Xing, Z., Li, P., Wu, S., Liu, C., Dai, D., Li, X., Zhang, L., Wang, D., Yang, Z., and Wang, Z. (2020). A perovskite-like LaSrGaO<sub>4</sub>: Mn<sup>2+</sup>, Nd<sup>3+</sup>, Yb<sup>3+</sup> NIR luminescent material for fluorescent temperature sensor. *J. Lumin.* 225, 117352. <https://doi.org/10.1016/j.jlumin.2020.117352>.

Xu, J., Miao, Y., Zheng, J., Wang, H., Yang, Y., and Liu, X. (2018a). Carbon dot-based white and yellow electroluminescent light emitting diodes with a record-breaking brightness. *Nanoscale* 10, 11211–11221. <https://doi.org/10.1039/c8nr01834k>.

Xu, J., Miao, Y., Zheng, J., Yang, Y., and Liu, X. (2018b). Ultrahigh brightness carbon dot-based blue electroluminescent LEDs by host-guest energy transfer emission mechanism. *Adv. Opt. Mater.* 6, 1800181. <https://doi.org/10.1002/adom.201800181>.

Xu, J.H., Dong, C., Ding, H.Z., and Bi, H. (2020b). Synthesis, luminescence mechanism and applications of carbon dots with afterglow. *Chinese J. Lumin.* 41, 1567–1578. <https://doi.org/10.37188/cjl.20200318>.

Xu, S., Chen, R., Zheng, C., and Huang, W. (2016). Excited state modulation for organic afterglow: materials and applications. *Adv. Mater.* 28, 9920–9940. <https://doi.org/10.1002/adma.201602604>.

Xu, X., Ray, R., Gu, Y., Ploehn, H.J., Gearheart, L., Raker, K., and Scrivens, W.A. (2004). Electrophoretic analysis and purification of fluorescent single-walled carbon nanotube fragments. *J. Am. Chem. Soc.* 126, 12736–12737. <https://doi.org/10.1021/ja040082h>.

Xu, Y., Liang, X., Zhou, X., Yuan, P., Zhou, J., Wang, C., Li, B., Hu, D., Qiao, X., Jiang, X., et al. (2019). Highly efficient blue fluorescent OLEDs based on upper level triplet-singlet intersystem crossing. *Adv. Mater.* 31, e1807388. <https://doi.org/10.1002/adma.201807388>.

Xu, Z., Sun, X., Ma, P., Chen, Y., Pan, W., and Wang, J. (2020a). A visible-light-excited afterglow achieved by carbon dots from rhodamine B fixed in boron oxide. *J. Mater. Chem. C Mater.* 8, 4557–4563. <https://doi.org/10.1039/c9tc05992j>.

Yang, J., Zhen, X., Wang, B., Gao, X., Ren, Z., Wang, J., Xie, Y., Li, J., Peng, Q., Pu, K., and Li, Z. (2018). The influence of the molecular packing on the room temperature phosphorescence of

purely organic luminogens. *Nat. Commun.* 9, 840–850. <https://doi.org/10.1038/s41467-018-03236-6>.

Yao, L., Zhang, S., Wang, R., Li, W., Shen, F., Yang, B., and Ma, Y. (2014). Highly efficient near-infrared organic light-emitting diode based on a butterfly-shaped donor-acceptor chromophore with strong solid-state fluorescence and a large proportion of radiative excitons. *Angew. Chem. Int. Ed. Engl.* 53, 2119–2123. <https://doi.org/10.1002/anie.201308486>.

Yen, W.M., Yamamoto, H., and Shionoya, S. (2007). *Phosphor Handbook, Second edition*.

Yuan, J., Tang, Y., Xu, S., Chen, R., and Huang, W. (2015). Purely organic optoelectronic materials with ultralong-lived excited states under ambient conditions. *J. Bull.* 60, 1631–1637. <https://doi.org/10.1007/s11434-015-0894-9>.

Yuan, T., Meng, T., He, P., Shi, Y., Li, Y., Li, X., Fan, L., and Yang, S. (2019). Carbon quantum dots: an emerging material for optoelectronic applications. *J. Mater. Chem. C Mater.* 7, 6820–6835. <https://doi.org/10.1039/c9tc01730e>.

Zhai, L., Ren, X.M., and Xu, Q. (2021). Carbogenic  $\pi$ -conjugated domains as the origin of afterglow emissions in carbon dot-based organic composite films. *Mater. Chem. Front.* 5, 4272–4279. <https://doi.org/10.1039/d1qm00019e>.

Zhang, Y., Wang, Y., Feng, X., Zhang, F., Yang, Y., and Liu, X. (2016). Effect of reaction temperature on structure and fluorescence properties of nitrogen-doped carbon dots. *Appl. Surf. Sci.* 387, 1236–1246. <https://doi.org/10.1016/j.apsusc.2016.07.048>.

Zhang, F., Feng, X., Zhang, Y., Yan, L., Yang, Y., and Liu, X. (2016a). Photoluminescent carbon quantum dots as a directly film-forming phosphor towards white LEDs. *Nanoscale* 8, 8618–8632. <https://doi.org/10.1039/c5nr08838k>.

Zhang, F., Wang, Y., Miao, Y., He, Y., Yang, Y., and Liu, X. (2016b). Optimal nitrogen and phosphorus codoping carbon dots towards white light-emitting device. *Appl. Phys. Lett.* 109, 083103. <https://doi.org/10.1063/1.4961631>.

Zhang, H., Liu, J., Wang, B., Liu, K., Chen, G., Yu, X., Li, J., and Yu, J. (2020a). Zeolite-confined carbon dots: tuning thermally activated delayed fluorescence emission via energy transfer. *Mater. Chem. Front.* 4, 1404–1410. <https://doi.org/10.1039/c9qm00549h>.

Zhang, H., Liu, K., Liu, J., Wang, B., Li, C., Song, W., Li, J., Huang, L., and Yu, J. (2020b). Carbon dots-in-zeolite via in-situ solvent-free thermal crystallization: achieving high-efficiency and ultralong afterglow dual emission. *CCS Chem.* 2, 118–127. <https://doi.org/10.31635/ccschem.020.201900099>.

Zhang, S., Yang, D., Shao, K., and Pan, Z.F. (2021). Progress in thermoluminescence spectroscopy for characterization of trap distribution in

persistent luminescence materials. *Laser & Optoelectronics Progress* 58, 72–83. <https://doi.org/10.3788/lop.202158.1516006>.

Zhang, X., Chen, L., Wei, Y.Y., Du, J.L., Yu, S.P., Liu, X.G., Liu, W., Liu, Y.J., Yang, Y.Z., and Li, Q. (2022). Cyclooxygenase-2-targeting fluorescent carbon dots for the selective imaging of golgi apparatus. *Dyes Pigm.* 201, 110213. <https://doi.org/10.1016/j.dyepig.2022.110213>.

Zhao, S., Wang, Z., Ma, Z., Fan, F., and Liu, W. (2020a). Achieving multimodal emission in Zn<sub>4</sub>B<sub>6</sub>O<sub>13</sub>: Tb<sup>3+</sup>, Yb<sup>3+</sup> for information encryption and anti-counterfeiting. *Inorg. Chem.* 59, 15681–15689. <https://doi.org/10.1021/acs.inorgchem.0c02019>.

Zhao, W.S., Li, X.X., Zha, H., Yang, Y.Z., Yan, L.P., Luo, Q., Liu, X.G., Wang, H., Ma, C.Q., and Xu, B.S. (2021). Controllable photoelectric properties of carbon dots and their application in organic solar cells. *Chin. J. Polym. Sci.* 40, 7–20. <https://doi.org/10.1007/s10118-021-2637-5>.

Zhao, W., Yan, L., Gu, H., Li, Z., Wang, Y., Luo, Q., Yang, Y., Liu, X., Wang, H., and Ma, C.Q. (2020b). Zinc oxide coated carbon dot nanoparticles as electron transport layer for inverted polymer solar cells. *ACS Appl. Energy Mater.* 3, 11388–11397. <https://doi.org/10.1021/acs.aem.0c02323>.

Zhao, Y., Mu, L., Su, Y., Shi, L., and Feng, X. (2017). Pt-Ni nanoframes functionalized with carbon dots: an emerging class of bio-nanoplatfoms. *J. Mater. Chem. B* 5, 6233–6236. <https://doi.org/10.1039/c7tb01678f>.

Zhao, Y., Shi, L., Fang, J., and Feng, X. (2015). Bio-nanoplatfoms based on carbon dots conjugating with F-substituted nano-hydroxyapatite for cellular imaging. *Nanoscale* 7, 20033–20041. <https://doi.org/10.1039/c5nr06837a>.

Zhou, W., Zhuang, J., Li, W., Hu, C., Lei, B., and Liu, Y. (2017). Towards efficient dual-emissive carbon dots through sulfur and nitrogen co-doped. *J. Mater. Chem. C Mater.* 5, 8014–8021. <https://doi.org/10.1039/c7tc01819c>.

Zhu, S., Meng, Q., Wang, L., Zhang, J., Song, Y., Jin, H., Zhang, K., Sun, H., Wang, H., and Yang, B. (2013). Highly photoluminescent carbon dots for multicolor patterning, sensors, and bioimaging. *Angew. Chem. Int. Ed. Engl.* 52, 3953–3957. <https://doi.org/10.1002/anie.201300519>.

Zhuo, Y., and Brgoch, J. (2021). Opportunities for next-generation luminescent materials through artificial intelligence. *J. Phys. Chem. Lett.* 12, 764–772. <https://doi.org/10.1021/acs.jpclett.0c03203>.

Zou, W.S., Ji, Y.J., Wang, X.F., Zhao, Q.C., Zhang, J., Shao, Q., Liu, J., Wang, F., and Wang, Y.Q. (2016). Insecticide as a precursor to prepare highly bright carbon dots for patterns printing and bioimaging: a new pathway for making poison profitable. *Chem. Eng. J.* 294, 323–332. <https://doi.org/10.1016/j.cej.2016.03.004>.